



저작자표시-동일조건변경허락 2.0 대한민국

이용자는 아래의 조건을 따르는 경우에 한하여 자유롭게

- 이 저작물을 복제, 배포, 전송, 전시, 공연 및 방송할 수 있습니다.
- 이차적 저작물을 작성할 수 있습니다.
- 이 저작물을 영리 목적으로 이용할 수 있습니다.

다음과 같은 조건을 따라야 합니다:



저작자표시. 귀하는 원저작자를 표시하여야 합니다.



동일조건변경허락. 귀하가 이 저작물을 개작, 변형 또는 가공했을 경우에는, 이 저작물과 동일한 이용허락조건하에서만 배포할 수 있습니다.

- 귀하는, 이 저작물의 재이용이나 배포의 경우, 이 저작물에 적용된 이용허락조건을 명확하게 나타내어야 합니다.
- 저작권자로부터 별도의 허가를 받으면 이러한 조건들은 적용되지 않습니다.

저작권법에 따른 이용자의 권리는 위의 내용에 의하여 영향을 받지 않습니다.

이것은 [이용허락규약\(Legal Code\)](#)을 이해하기 쉽게 요약한 것입니다.

[Disclaimer](#)

August 2011

Master's Thesis

Mechanical properties and  
Microstructure of Friction Stir  
Welds for high melting  
temperature materials

Graduate School of Chosun  
University

Department of naval architecture

Ki-Sang Bang

# Mechanical properties and Microstructure of Friction Stir Welds for high melting temperature materials

고융점 소재에 대한 마찰교반용접부의  
기계적 성질 및 미세조직

August 25, 2011

Graduate School of Chosun  
University

Department of naval architecture

Ki-Sang Bang

# Mechanical properties and Microstructure of Friction Stir Welds for high melting temperature materials

Advisor: Professor Hee-Seon Bang

A Thesis submitted for the degree of  
Master of Engineering

August 2011

Graduate School of Chosun  
University

Department of naval architecture

Ki-Sang Bang

Ki-Sang Bang's master thesis  
is certified

Committee Chair Chosun Univ. Prof. Han-Sur Bang

Member Chosun Univ. Prof. Hee-Seon Bang

Member KITECH Prof. Kwang-Jin Lee

May 2011

Graduate School of Chosun University

# Part 1

## CONTENTS

List of Tables .....	III
List of Figures .....	IX
Abstract .....	VIII

### Chapter 1. Introduction

1 . 1 Experimental background & Purpose .....	1
---	---

### Chapter 2. Theoretical background

2 . 1 Principles and characteristics of FSW .....	3
2.1.1 Principle of FSW .....	3
2.1.2 Characteristics of FSW .....	8
2 . 2 characteristics of object materials .....	9

### Chapter 3. Experiment method of friction stir welding process

3 . 1 Details of friction stir welding .....	11
3.1.1 Specification of friction stir welding machine ..	11

3 . 2 Tool geometry .....	13
3 . 3 Friction stir welding condition .....	16
3 . 4 Experiment method .....	19
3.4.1 Tensile test .....	19
3.4.2 Hardness test .....	21
3.4.3 Impact test .....	22
3.4.4 Micro structure analysis .....	24

## Chapter 4. Result & disscusion

4 . 1 Bead appearance of each welding condition ..	25
4 . 2 Mechanical properties of friction stir welds ...	27
4.2.1 Tensile test results .....	27
4.2.2 Hardness test results .....	30
4 . 3 Microstructure of friction stir welds .....	31

제 5 장 Conclusion .....	36
------------------------	----

Reference .....	37
-----------------	----

# List of Tables

Table 2.1	Chemical compositions of SS400 .....	9
Table 2.2	Mechanical properties of SS400 .....	9
Table 2.3	Chemical compositions of AA6061-T6 and Ti-6Al-4V .....	9
Table 2.4	Mechanical properties of AA6061-T6 and Ti-6Al-4V .....	10
Table 3.1	2-dimensional precision FSW machine of its specification .....	11
Table 3.2	Tool appearance and Tool geometry .....	14
Table 3.3	Mechanical properties of conventional and developed tool materials .....	14
Table 3.4	Welding condition during FSW .....	17
Table 4.1	Bead appearance by 400RPM .....	25
Table 4.2	Bead appearance by 400RPM .....	26



# List of Figures

Fig. 1.1 Schematics of materials according to Melting temperature	2
Fig. 2.1 Schematics drawing of Friction Stir Welding process	4
Fig. 2.2 Microstructural regions in FSWed alloys	6
Fig. 2.3 Comparison of FSW and conventional welding process; welding appearance after weld(a) and mechanical properties(b)	7
Fig. 3.1 Tool rotating direction during FSW	12
Fig. 3.2 Sintering process for applicaton of FSW Tool	13
Fig. 3.3 Schematic illustrating of friction stir welding	16
Fig. 3.4 Schematic diagram of FSW process	18
Fig. 3.5 Tensile test of Friction stir welded SS400	19
Fig. 3.6 Dimension of tensile test specimen	20
Fig. 3.7 Vickers hardness test machine and specimen	21
Fig. 3.8 Impact test machine and dimension	26
Fig. 3.9 Optical microscopy	26
Fig. 4.1 Tensile strength of Rotation speed_400RPM	27
Fig. 4.2 Fractured specimens agter tensile test_400RPM	28
Fig. 4.3 Tensile strength of Roation speed_600RPM	29
Fig. 4.4 Fractured specimens agter tensile test_600RPM	29
Fig. 4.5 Hardness profile of friction stir welded SS400	30
Fig. 4.6 Microstructure of friction stir welded SS400 on rotating speed 400RPM and traveling 3mm/s	31
Fig. 4.7 Microstructure of friction stir welded SS400 on rotating speed 400RPM and traveling 8mm/s	32
Fig. 4.8 Microstructure of friction stir welded SS400 on rotating speed 600RPM and traveling 8mm/s	33
Fig. 4.6 SEM observation of fracture surface and EDAX result_BM	34
Fig. 4.6 SEM observation of fracture surface and EDAX result_weld zone	35

## Part 2

# CONTENTS

List of Tables .....	VI
List of Figures .....	VII
Abstract .....	IX

## Chapter 1. Introduction

1 . 1 Background & Purpose .....	39
----------------------------------	----

## Chapter 2. Experimental procedure

2 . 1 Expeirmental procedure .....	41
------------------------------------	----

## Chapter 3. Result and discussion

3 . 1 Mechanical properties .....	44
3 . 2 Interfacial microstructure .....	46

Chapter 4. Conclusion .....	52
-----------------------------	----

Reference .....	53
-----------------	----

# List of Tables

Table 2.1 Chemical composition of AA6061-T6 and Ti-6Al-4V base metals(at%) .....	41
Table 2.2 Mechanical propertisof AA6061-T6 and Ti-6Al-4V base metals(at%) .....	41

# List of Figures

Fig. 2.1 Schematic illustration of friction stir welding process between AA6061-T6 and Ti-6Al-4V .....	42
Fig. 2.2 Schematic illustration of joint interface .....	42
Fig. 3.1 Hardness profile for the welding cross-section .....	44
Fig. 3.2 Strain-Stress curve of friction stir welds between and AA6061-T6 and Ti-6Al-4V .....	45
Fig. 3.3 The cross-section image of friction stir welded AA6061-T6 and Ti-6Al-4V(a) and the optical microscopy(OM) images of the cross-section(b-g). .....	46
Fig. 3.4 SEM images of probe root area(a), middle area(b), tip area(c) in the weld interface .....	47
Fig. 3.5 SEM images for fracture surface (a) and probe tip area (b)	48
Fig. 3.6 TEM specimens fabricated by FIB .....	48
Fig. 3.7 bright dark filed images of probe root area(a) and probe tip area(b) .....	49
Fig. 3.8 High angle annular dark field(HAADF) images and elements mapping of probe root area in FSW welds .....	49
Fig. 3.9 HAADF image and elements mapping of probe tip area ...	51

# Part 1

## ABSTRACT

### SS400에 대한 마찰교반용접부의 기계적 성질 및 미세조직 평가

Bang, Ki-Sang

Advisor : Prof. Bang, Han-sur, Ph.D.

Department of Naval Architecture and  
Ocean Engineering ,

Graduate School of Chosun University

마찰교반용접(Friction Stir welding, FSW)는 1991년 영국TWI에서 개발한 고상접합법으로, probe와 shoulder로 구성되는 Tool고속으로 회전시키면서 용접하고자 하는 재료에 삽입하여 재료의 표면과 내부에서 발생하는 마찰열을 이용하여 재료를 연화함과 동시에 고온 소성유동을 일으켜 툴의 좌우에 배치된 재료의 일부를 상호간에 맞은편 영역에 교반혼입시켜 접합을 실현하는 고상 접합 방법이다. 이 접합방법은 기존의 용융 용접 방법들과 비교하여 발열이 최소한으로 억제되어, 접합후 열에 의한 변형이 현저히 감소하고, 접합후의 결함도 거의 발생되지 않으며, 강력한 소성변형에 의해 접합부 조직이 모재보다 미세화 되는 등의 이점이 많아 개발된 지 십수년밖에 지나지 않았음에도 불구하고, 이미 자동차, 철도차량, 선박 및 항공우주분야 등 다양한 분야의 제품에 적용되고 있으며, 최근에는 동, 타이타늄, 고장력강 등으로 적용을 확대하기 위한 연구가 진행되고 있다. 하지만 기존의 툴을 사용하여 고용점소재 즉 타이타늄, 고장력강에 마찰교반용접을 적용시킬 경우, 툴의 마모가 발생하여 건전한 접합체를 얻을 수가 없다.

그리하여 본연구에서는 Spark Plasma Sintering process(SPS,방전유도소결법)을 Tool 재료 개발에 적용시켜, 고용점 소재에 대한 마찰교반용접의 최적화 공정을 개발하였다. 아울러 용접부에 대한 기계적성질을 평가하기 위해 인장시험, 경도시험을 실시하였고, 미세조직은 광학현미경과, 주사전자현미경을 사용하여 평가하였다.

## Part 2

### ABSTRACT

#### AA6061-T6 알루미늄합금과 Ti-6Al-4V 타이타늄 합금 이종 마찰교반용접부에 대한 미세조직 및 기계적 성질

Bang, Ki-Sang

Advisor : Prof. Bang, Han-sur, Ph.D.

Department of Naval Architecture and

Ocean Engineering ,

Graduate School of Chosun University

Ti합금은 경량합금이면서도 강도가 우수할 뿐 아니라 내식성 또한 우수하여 항공기의 각종 구조부품 및 기능성부품 소재로의 적용확대가 기대되고 있다. 이에 따라 기존의 항공기 구조용 소재인 Al합금과 Ti합금에 대한 이종금속의 용접 및 접합이 중요한 기술적 요인으로 주목을 받고 있다. Arc 및 Laser 용접등과 같은 기존의 용융용접 방법을 적용할 경우, 용접부에  $Ti_3Al$ ,  $TiAl$ ,  $TiAl_2$ ,  $Ti_2Al_5$  및  $TiAl_3$  등과 같은 취약한 금속간 화합물이 생성하여 강도 특성이 현저히 저하하는 등 건전한 접합체를 얻기가 어려운 것이 현실이다. 이에 대표적인 고장접합 방법인 마찰교반용접에 관심이 집중되고 있으며, 미국과 유럽등 항공기 제조업체를 중심으로 기초 연구가 진행되고 있다. 이 연구들은 마찰교반접합 공정 및 강도 등의 물리적 특성에 관한 내용이 대부분이다. 그러나 이종금속의 경우, 건전한 물리적 특성을 얻기 위해서는 접합부 특히 접합계면 미세조직에 대한 연구와 조직제어가 필수적으로 선행되어야한다. 본 연구에서는 Al합금과 Ti합금 판재에 대한 마찰교반접합부 계면 미세조직의 형성을 검토하기 위하여 고강도 Al합금인 6061-T6 및 상용화된 Ti 합금인 Ti-6Al-4V판재에 대하여 맞대기 마찰교반용접을 실시한 후, 접합 계면부에 대한 상세한 조직관찰 및 성분분포를 조사하였다.

# Part 1

## Chapter 1

### Introduction

#### 1 . 1 Experimental background and purpose

There are many kinds of approach to meet the demands where consider the environmental problem and the resource exhaustion. Therefore, The highest performance and concurrent weight and cost reduction became more important in transportation industries such as automobile, aircraft, vessel and railway vehicle. So many researchers are focusing on lightweight structures which are economical and environmentally. Therefore, manufactures are developing the lighter materials with a higher mechanical properties by various methods like design and processing by alloy.

Steel joints are used in structure where high strength are desirable. Riveting and bimetallic strip joining techniques for steel joint increases manufacturing cost and require more work time.

To solve this problem, Friction stir welding process is a novel solid state joining process that was invented in 1991. FSW can avoid many problems associated with conventional fusion welding methods, there by producing defect free welds with excellent properties, even in some materials with poor weldability.

Due to its many advantages, FSW attracts a great deal of attention in the industrial fields, and is successfully applied to the joining of various aluminum alloy, magnesium and copper alloys. In recent years, FSW of high melting temperature materials such as steels and titanium and nickel alloys has become a research carefully. However, that kinds of joint are difficult to obtain high melting temperature materials. especially steels, titanium, nickel and their alloys, because of tool limitation. Thus, to

overcome this problem for joining high melting temperature materials, new tool materials was intended by spark plasma sintering process. Hence, this work intend to establish the possibility of joining high melting temperature materials.

mechanical properties and microstructure of friction stir welds are studied.

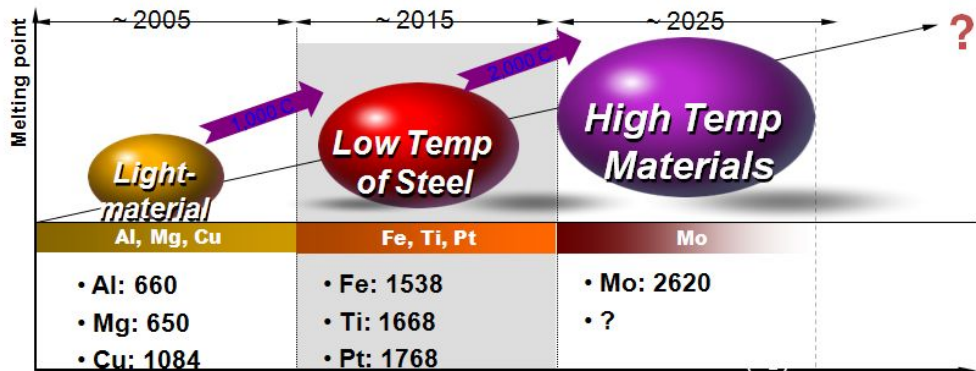


Fig. 1.1 Schematics of materials according to Melting temperature



## Chapter 2

# THEORETICAL BACKGROUND

### 2 . 1 Principles and characteristics of FSW

#### 2 . 1 . 1 Principle of FSW

Friction stir welding was invented at the TWI in 1991 as a solid-state joining process and was initially applied to lightweight metals. The concept is remarkably simple. A nonconsumable rotating tool with a designed probe and shoulder is inserted into the edges of sheets or plates to be joined. Fig 2.1 shows schematic drawing of Friction Stir Welding process. Most definitions are self-explanatory, but advancing side and retreating side definitions require a brief explanation. Advancing side and retreating side orientations require knowledge of the tool rotation and travel direction. In Fig. 2.1 the FSW tool rotates in the counterclockwise direction and travels into the page. The advancing side is on the right, where the tool rotation direction is the same as the tool travel direction, and the tool retreating side is on the left, where the tool rotation direction is opposite the tool travel direction.

The tool serves three primary functions, that is, heating of the workpiece, movement of material to produce the joint, and containment of the hot metal beneath the tool shoulder. Heating is created within the workpiece both by friction between the rotating tool probe and shoulder and by severe plastic deformation of the workpiece. The localized heating softens material around the probe and, combined with the tool rotation and translation, lead to movement of material from the front to the back of the probe, thus filling the hole in the tool with as the tool moves forward.

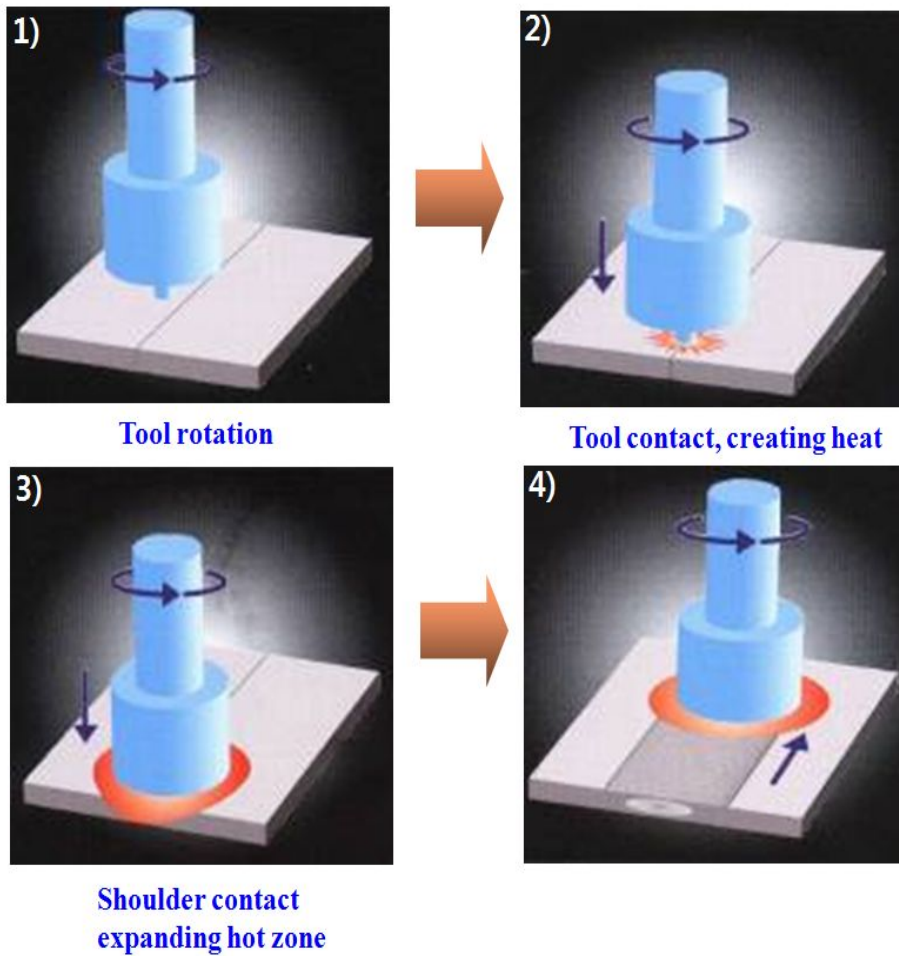
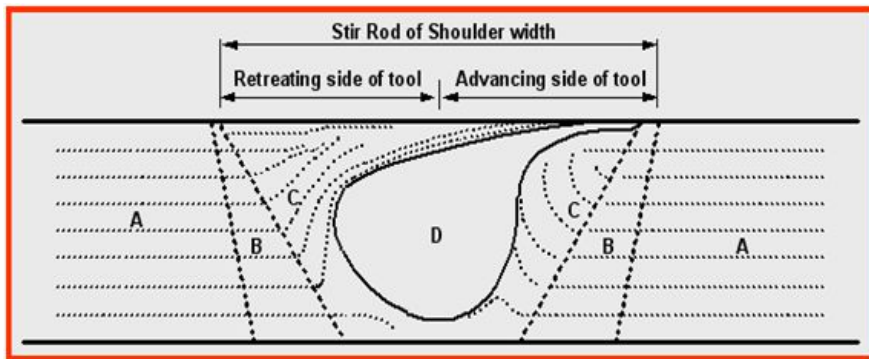


Fig. 2.1 Schematics drawing of Friction Stir Welding process

The system divides the weld zone into distinct regions, as follow:

- Stir Zone: The fully recrystallized area, sometimes called the weld nugget, refers to the zone previously occupied by the tool probe. The term stir zone is commonly used in friction stir processing, where large volumes of material are processed.
  
- Thermomechanically affected zone(TMAZ): In this region, the FSW tool has plastically deformed the material, and the heat from the process will also have exerted some influence on the material. In the case of aluminium, it is possible to obtain significant plastic strain without recrystallization in this region, and there is generally a distinct boundary between the recrystallized zone(weld nugget) and the deformed zones of the TMAZ
  
- Heat affected zone(HAZ): In this region, which lies closer to the weld center, the material has experienced a thermal cycle that has modified the microstructure and/or the mechanical properties. However, there is no plastic deformation occurring in this area.



A: BM (Base Metal)

B: HAZ (Heat Affected Zone; affected by heat generated during FSW )

C: TMAZ (Thermomechanically Affected Zone; contains material that interacts indirectly with the tool , plastically deformed with partial recrystallization)

D: SZ (Stir Zone; contains material that interacts directly with the tool, dynamically recrystallized)

**Fig. 2.2 Microstructural regions in FSWed alloys**

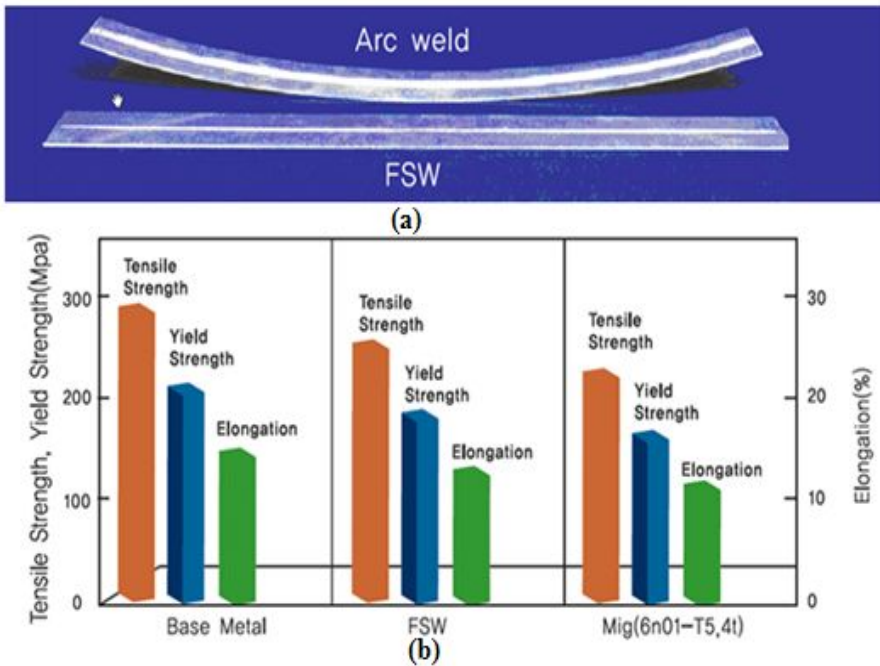


Fig. 2.3 Comparison of FSW and conventional welding process; welding appearance after weld(a) and mechanical properties(b)

## 2 . 1 . 2 Characteristics of FSW

### 1) Advantage of Friction stir welding

- Good mechanical properties in the as welded condition improved safety due to the absence of toxic fumes or the spatter of molten material
- No consumable –conventional steel tools can weld over 1000m of aluminum and no filler or gas shield is required for aluminum.
- Easily automated on simple milling machines– lower operation costs and less training.
- Can operate in all positions(horizontal, vertical, etc), as there is no weld pool
- Generally good weld appearance and minimal thickness under/over –matching, thus reducing the need for expensive machining after welding.
- Low environmental impact.

### 2) Disadvantages of Friction stir welding

- Exit hole left when tool is withdrawn.
- Large down forces required with heavy–duty clamping necessary to hold the plates together.
- Less flexible than manual and arc processes (difficulties with thickness variations and non–linear welds)
- often slower traverse rate than some fusion welding techniques although this may be offset if fewer welding passes are required.

## 2 . 2 Characteristics of object materials

The materials used for this study are AA6061-T6 and Ti-6Al-4V and SS400. To minimize the mechanical effect in welds such as contraction and expansion in weldment, specimens with dimension  $200 \times 100 \times 5$  and  $200 \times 100 \times 2$  was fabricated to conduct the welding experiment.

**Table 2.1 Chemical compositions of SS400**

Materials	Chemical composition(wt%)				
	C	Si	Mn	P	S
SS400	0.14	0.009	0.67	0.01	0.003

**Table 2.2 Mechanical properties of SS400**

	Yield stress(MPa)	UTS(MPa)	Elongation(%)
SS400	310	350	42

**Table 2.3 Chemical compositions of AA661-T6 and Ti-6Al-4V**

Material	Al	Si	Mg	Cu	Fe	Mn	Others
AA6061-T6	Balance	0.56	0.98	0.31	0.29	0.05	0.04
Material	Ti	Al	Ni	C	V	Fe	Others
Ti-6Al-4V	Balance	6.62	0.05	0.10	3.95	0.40	0.035

**Table 2.4 Mechanical properties of AA661-T6 and Ti-6Al-4V**

	<b>Yield stress(MPa)</b>	<b>UTS(MPa)</b>	<b>Elongation</b>
AA6061-T6	310	342	17
Ti-6Al-4V	880	950	14

Chemical compositions and mechanical properties of SS400, AA6061-T6 and Ti-6Al-4V are shown in Table 2.1, 2.2, 2.3 and 2.4, respectively.

AA6061-T6 has good mechanical properties and exhibits good weldability, and thus have been applied widely in construction of aircraft structures and automotive parts.

Ti-6Al-4V has high specific strengths and good erosion resistance, and it has been applied in the aerospace, chemical and nuclear industries.



# Chapter 3

## EXPERIMENT METHOD OF FRICTION STIR WELDING PROCESS

### 3 . 1 Details of friction stir welding

#### 3.1.1 Specification of Friction stir welding machine

The present study used friction stir welding machine fabricated by WINXEN Co. Table 3.1 shows specification of friction stir welding machine. As the table, stroke of X, Y and Z axis is 1600mm, 1800mm, 360mm, respectively. Maximum rotation speed and load capacity is 3000RPM, 2000kgf. Temperature telemetry and cooling system is available.

Table 3.1 2–dimensional precision FSW machine and its specification


FSW machine	Item		Specification	
	X-axis	Stroke	1,600mm	
		Speed	Max. 2,800 mm/min (3.2kw)	
	Y-axis	Stroke	1,800mm	
		Speed	Max. 2,800mm/min (3.2kw)	
	Z-axis	Stroke	360mm	
		Speed	Max. 2,800mm/min (5.5kw)	
	Turn Axis			1~20RPM(2.1kw)
	Spindle Speed			Max. 3,000RPM (22kw)
	Tilting angle			Max. 5°
	Pressure Load			Max. 2,000kgf
	Temperature Telemetry System			Available
	Cooling System			Available

Fig 3.1 shows Tool rotating direction during FSW. The inserting position of probe is zero offset position.

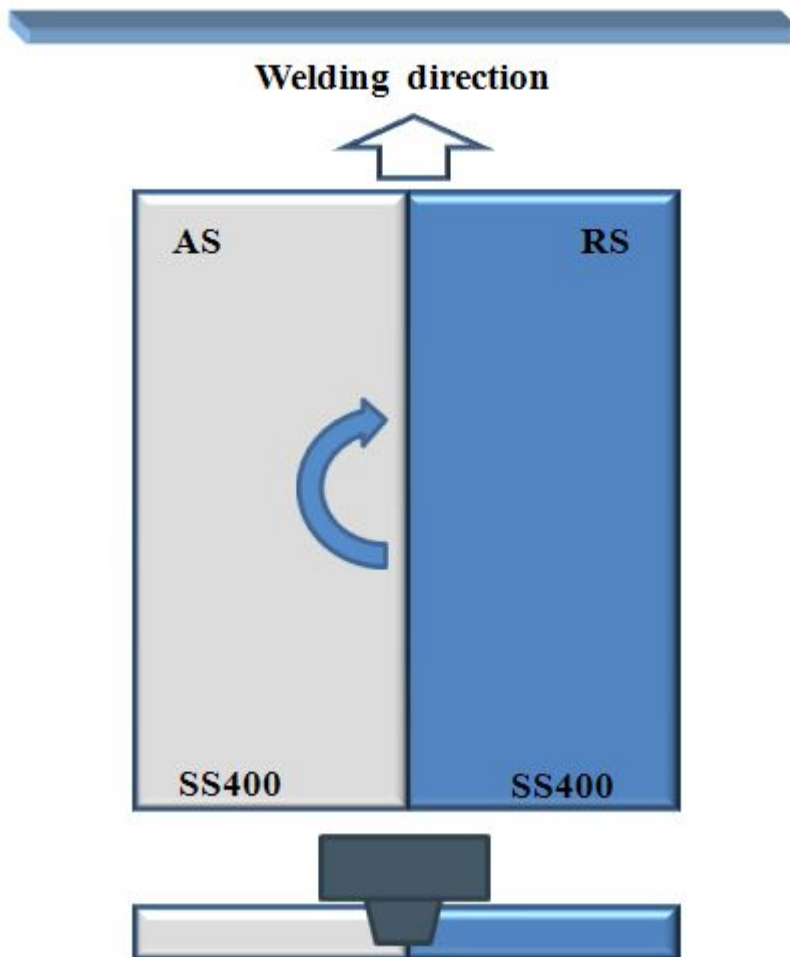
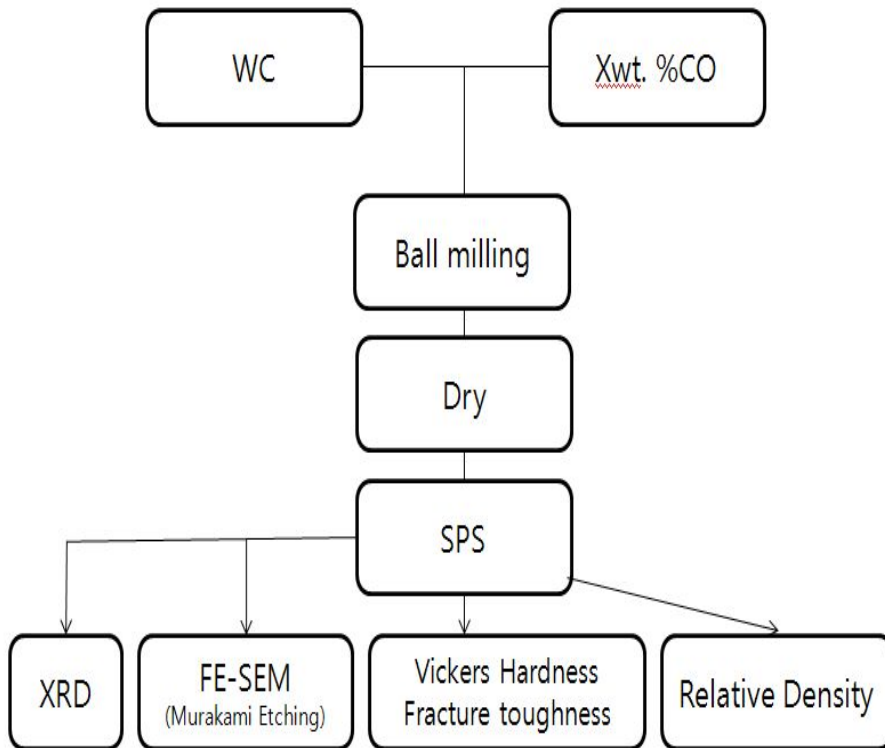


Fig. 3.1 Tool rotating direction during FSW

### 3 . 2 Tool geometry

In order to welding steel alloy, new tool material have been developed.

Fig. 3.2 shows spark plasma sintering process to apply FSW tool



**Fig. 3.2 Sintering process for applicaton of FSW Tool**

The tool materials is made of XWt% tungsten carbide fabricated by SPS . In order to prevent the tool wear-resistant, AlTiN coating was conducted by AIP process. Tool probe shape is smooth concave type and shoulder is designed to obtain the proper mixing at the stir zone with good plastic flow of metal. The shoulder is made concave with 3° clearance to take as an escape volume for the material displaced by the probe during plung action. The dimensions of shoulder and probe and tool shape to obtain substantial improvements in productivity and quality is shown Table 3.2.

Table 3.2 Tool appearance and Tool geometry

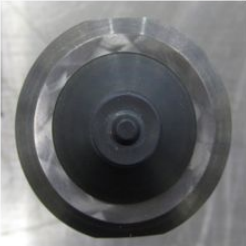
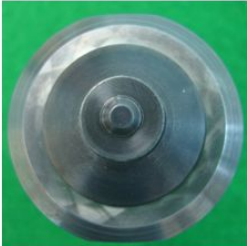
Before Welding	After Welding	Material	WC-x% CO
		Probe diameter(mm)	3~5
		Probe length(mm)	1.6
		Shoulder diameter(mm)	11

Table 3.3 Mechanical properties of Conventional and Developed tool material

	Conventional tool material	Developed tool material
Hardness value	1500HV	2100HV
Fracture toughness	$18MPa.m^{1/2}$	$10.6MPa.m^{1/2}$

Table 3.3 shows mechanical properties of conventional and developed tool

material.

$$K_{IC} = 0.016 (E/H)^{1/2} P / C^{3/2} \quad (1)$$

Developed tool material has a higher hardness value than conventional tool material. The hardness and fracture toughness were about 2100HV and  $10.6MP \cdot m^{1/2}$ , respectively.

### 3 . 3 Friction stir welding condition

The important variations of Friction stir welding are rotating speed, traveling speed, offset from weld line and Rotating direction of Tool. In case of Conventional dissimilar and similar friction stir welding process, sound weldability could not be obtained because of probe limitation. It has been reported that conventional tool materials could not weld to high melting temperature materials. Thus, the tool material was developed to apply welding about high melting materials and optimize friction stir welding condition in the present study. Fig. 3.3 shows schematic illustrating of the friction stir welding.

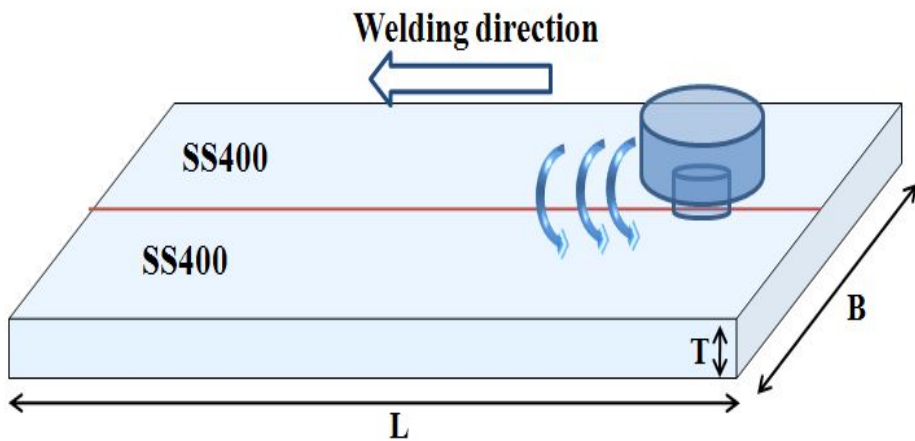


Fig. 3.3 Schematic illustrating of friction stir welding

Table 3.4 Welding condition during FSW

Welding condition		Values
FSW	Rotation speed(RPM)	400~800
	Welding speed(mm/s)	3~10
	Shoulder dia.(mm)	Ø11
	Pin dia.(mm)	Ø3~5
	Room temperature	20°
	Tilt angle	3°

Rectangular plates 2 and 5 mm thick, 20 mm long and 100 mm wide were butt welded. The tool had a shoulder diameter of 11 mm and a 4 mm probe diameter. The probe length was 1.6, 4.5 mm and the tool was tilted 3° towards the welding direction. The rotation speeds were 400~800RPM and the welding speeds were 3~10mm/s. The microstructure of each FSW joint was observed by optical microscopy and scanning electron microscopy (SEM).

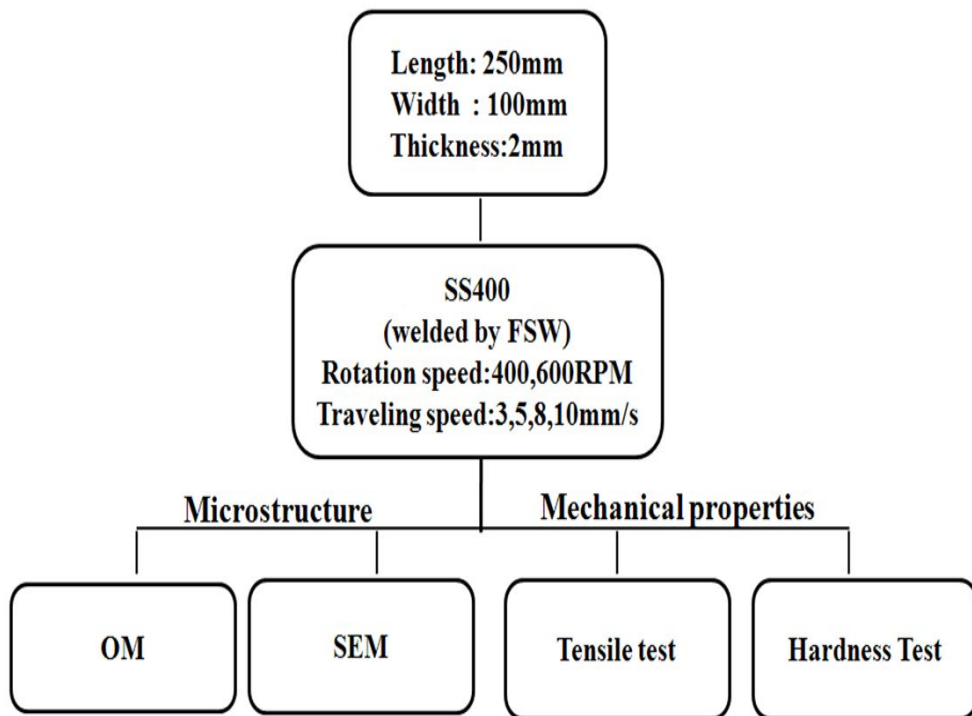


Fig. 3.4 schematic diagram of FSW process



## 3 . 4 Experimental method

### 3.4.1 Tensile test

Tensile test was carried out with Dongil-Simaz universal TestingMachine (EHF-EG200KN-40L) using WINSERVO program. Fig. 3.5 shows the EHF-EG200KN-40L and tensile testing setup.

The specimens are fabricated in accordance with the japan strandards. The specimens dimensions are shown in Fig. 3.6. Tensile test was conducted with load speed 0.05mm/sec and stress-strain curve was obtained.

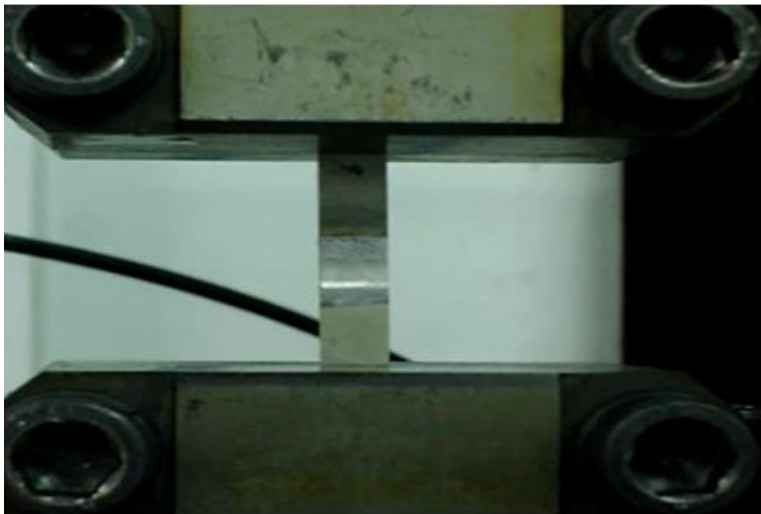


Fig. 3.5 Tensile test of Friction stir welded SS400

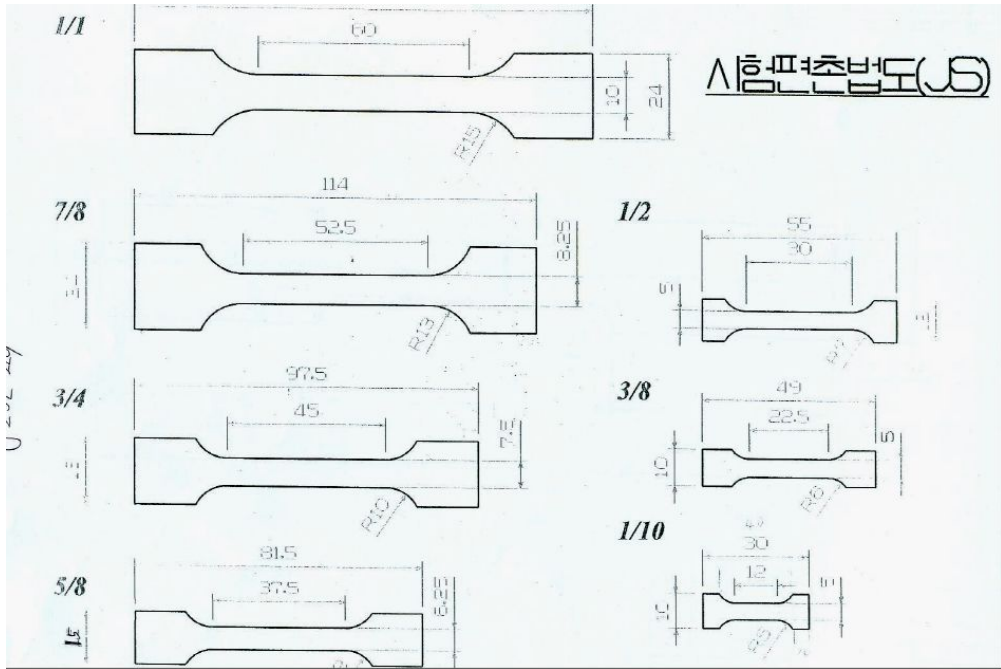


Fig. 3.6 Dimension of tensile test specimen

### 3.4.2 Hardness test

The hardness test of welded specimen was measured using AKASHI HM-112 vickers Hardness tester as shown in Fig. 3.7. The indenter employed in the vickers test was a square-based pyramid whose opposite sides meet at the apex at an angle of  $136^\circ$  with load 500g applied for 10 sec.

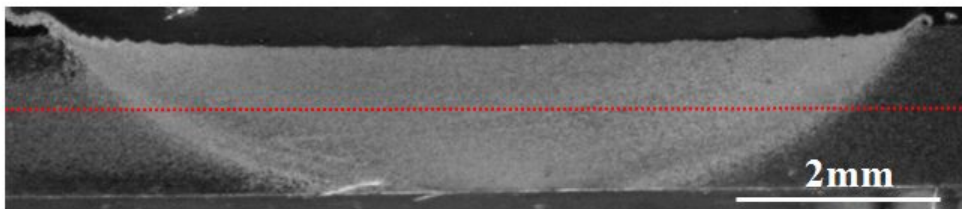


Fig. 3.7 Vickers hardness test machine and specimen

### 3.4.3 Impact test

The Charpy impact test, also known as the Charpy v-notch test, is a standardized high strain-rate test which determines the amount of energy absorbed by a material during fracture. This absorbed energy is a measure of a given material's toughness and acts as a tool to study temperature-dependent brittle-ductile transition. It is widely applied in industry, since it is easy to prepare and conduct and results can be obtained quickly and cheaply. But a major disadvantage is that all results are only comparative.

The test was developed in 1905 by the French scientist Georges Charpy. It was pivotal in understanding the fracture problems of ships during the Second World War. Today it is used in many industries for testing building and construction materials used in the construction of pressure vessels, bridges and to see how storms will affect materials used in building.

$$* h_1 = L \{1 + \cos (180^\circ - \alpha)\}$$

$$* h_2 = L (1 - \cos \beta)$$

$$* h = h_1 - h_2 = L \{\cos (180^\circ - \alpha) + \cos \beta\} = L (-\cos \alpha + \cos \beta)$$

$$* E = Wh = WL \{\cos \beta - \cos \alpha\}$$

$$\text{Impact value } U = E/A$$

$$\text{Therefore, } U = WL (\cos \beta - \cos \alpha) / A \text{ [kgf-m/cm}^2\text{]}$$

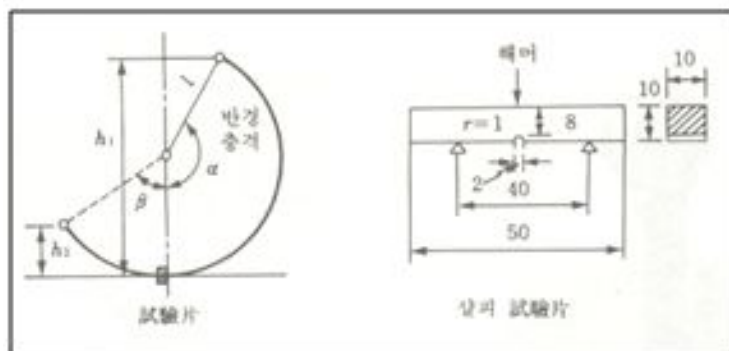


Fig. 3.8 Impact test machine and dimension

### 3.4.5 Microstructure analysis

The cross section of FSWed specimen was cut perpendicular to the welding direction(WD). It was polished with 1 and 3 $\mu$ m diamond suspension. Alumina powder was used as the final polishing solution, and then was chemically etched to observe the microstructure and macro of the joint.

The prepared specimen was mounted on OLYMPUS optical microscopy to observe the microstructure as shown in Fig. 3.9



Fig. 3.9 Optical microscope

## Chapter 4 Results and discussion

### 4 . 1 Bead appearandce of each welding condition

Table 4.1 Bead appearances by 400RPM





Rotation Speed(RPM)	Traveling Speed(mm/s)	Bead appearance
400	3	
400	5	
400	8	
400	10	

Table 4.1 shows bead appearances of rotating speed 400RPM. No defect was found in appearance of friction stir welds. However, burr was observed in region affected by shoulder. To overcome this problem, Z axid of tool have to be varied.

Table 4.2 Bead appearances by 600RPM



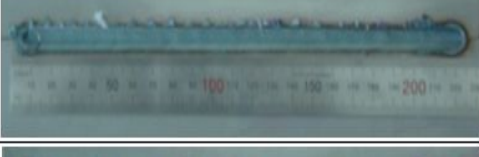
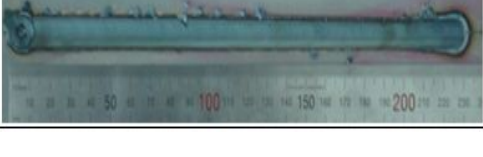
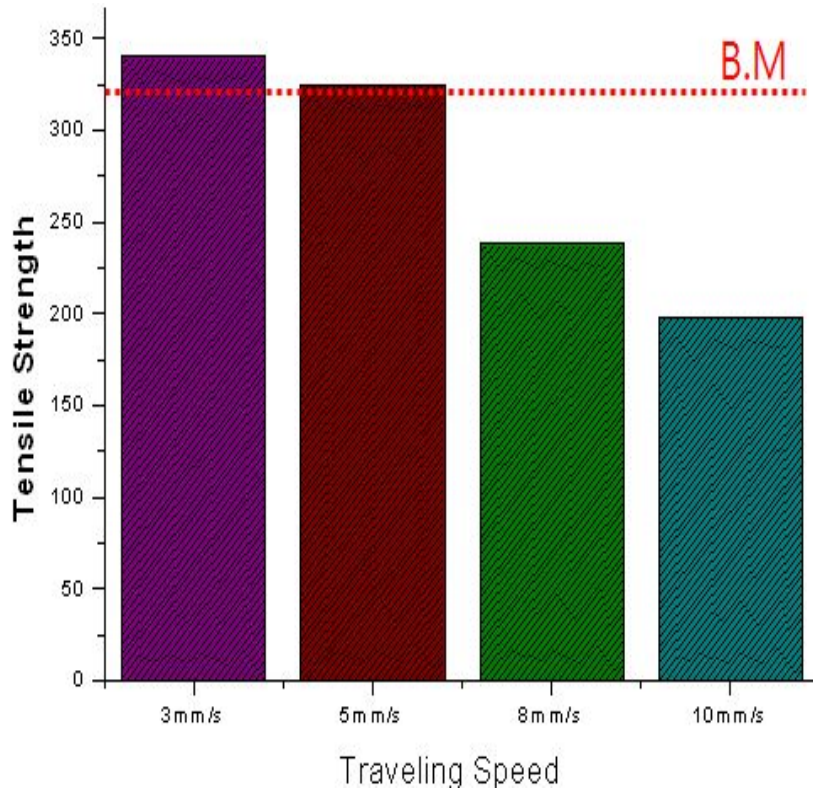
Rotation Speed(RPM)	Traveling Speed(mm/s)	Bead appearance
600	3	
600	5	
600	8	
600	10	

Table 4.2 shows bead appearances of rotating speed 400RPM. No defect was found in appearance of friction stir welds. However, burr was observed in region affected by shoulder. To overcome this problem, Z axid of tool have to be varied. Appearances of friction stir welds by 600RPM are clear better than appearance by rotating speed 400RPM.



## 4 . 2 Mechanical properties of friction stir welds

### 4 . 2. 1 Tensile test results



**Fig. 4.1 Tensile strength of Rotation Speed\_400RPM**

Fig. 4.1 shows tensile strength of friction stir welds that join to welding condition of rotating speed 400RPM and traveling speed 3, 5 ,8 and 10mm/s. For a given process parameter combination, variation in ultimate tensile strength (UTS) was found to be less than 2%.

However, significant differences, ranging from 200 MPa to 325 MPa, were

observed in UTS among the various welds, indicating that the process parameters have a strong bearing on the quality of joints. Among the

four weld samples, Samples 3 and 10mm/s showed the lowest (200 MPa) and highest (325 MPa) UTS values, respectively. All the samples were found to fracture in the weld region and base metal as shown in Fig. 4.2.

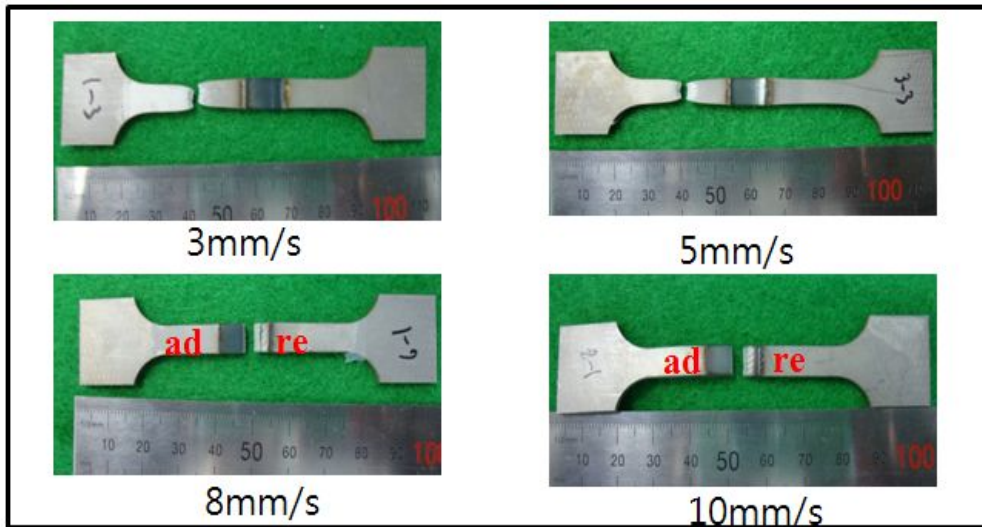


Fig. 4.2 Fractured specimens after tensile test\_Rotation speed 400RPM

Fig. 4.3 shows tensile strength of friction stir welds that join to welding condition of rotating speed 600RPM and traveling speed 3, 5, 8 and 10mm/s.

However, similar aspect, ranging from 300 MPa to 325 MPa, were observed in UTS among the various welds, indicating that the process parameters have a strong bearing on the quality of joints. Among the four weld samples, Samples 3 and 10mm/s showed the lowest (300 MPa) and highest (325 MPa) UTS values, respectively. All the samples were found to fail in the base metal as shown in Fig. 4.4.

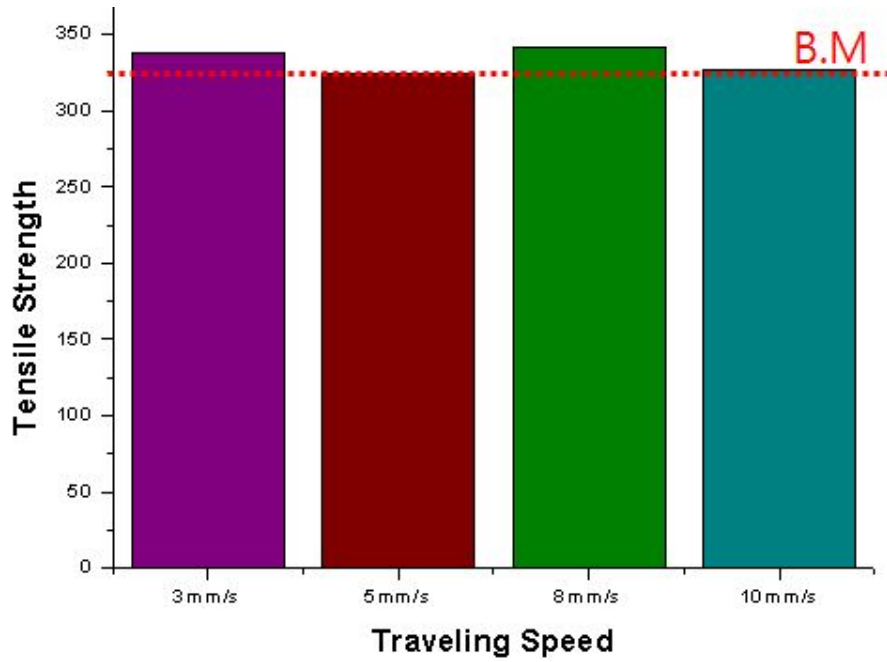


Fig. 4.3 Tensile strength of Rotation Speed\_600RPM

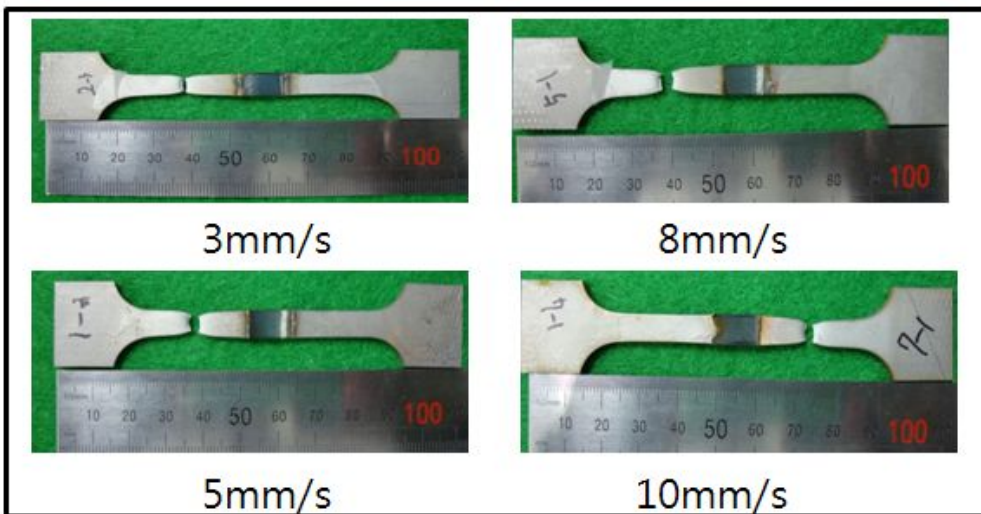


Fig. 4. 4 Fractured specimens after tensile test\_Rotation speed 600RPM

## 4 . 2 . 2 Hardness test results

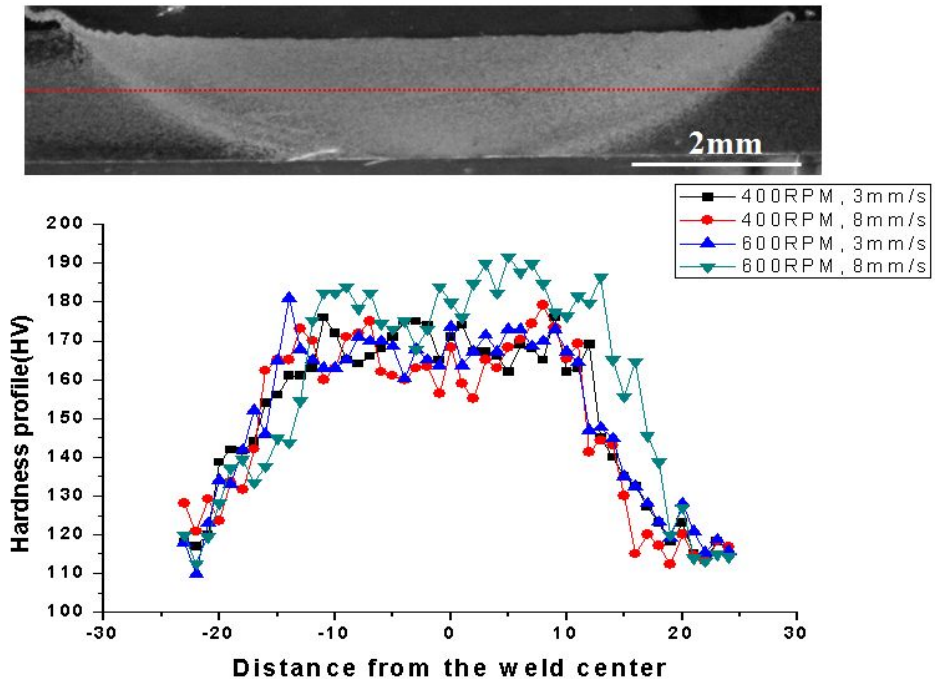


Fig. 4. 5 Hardness profile of Friction stir welded SS400

The hardness profile of Friction stir welds is shown in Fig. 4.5. Vickers microhardness measurements were made across the weld on each of rotating speed 400, 600RPM, and traveling speed 3, 8mm/s to see how the process affected strengthening precipitation in the three microstructural zones of the weld. The hardness profile can be seen to be more or less symmetric about the weld interface. There is a significant drop in hardness in the HAZ and TMAZ regions. On the rotating side, the TMAZ hardness was found to be higher than the HAZ hardness. In the SZ, considerable increase in hardness was found compared to HAZ.

### 4 . 3 Microstructure of friction stir welds

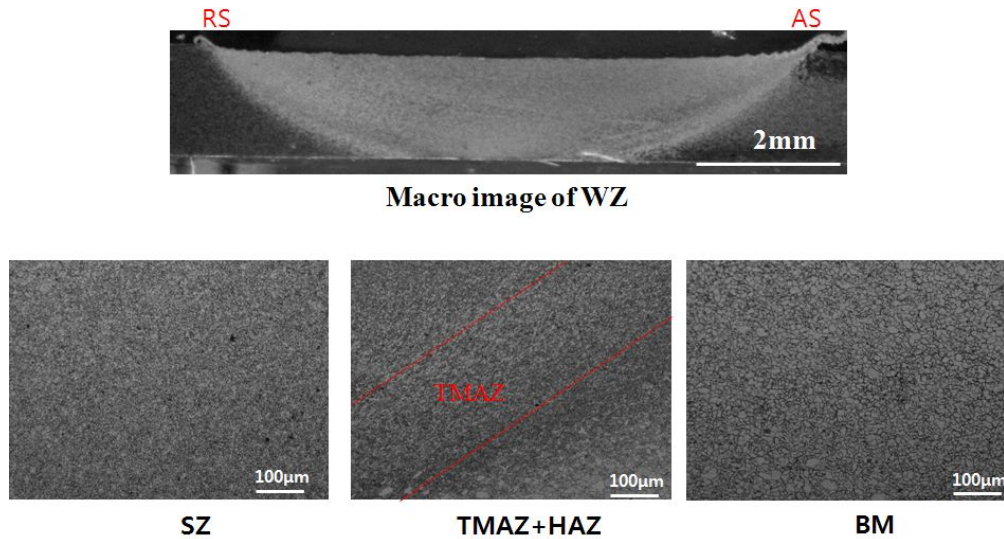


Fig. 4.6 Microstructure of friction stir welded SS400 on rotating speed 400RPM and traveling speed 3mm/s

Fig. 4.6 shows microstructure of friction stir welded SS400 on rotating speed 400RPM and traveling speed 3mm/s. No defect was observed in weld zone. As the observation result of optical microscopy, grain size of the BM evaluated about 10~20 µm. However, On the HAZ region was observed to grain coarsening in comparable with BM. Unrecrystallized grain structure can be retained in the TMAZ, which represents the extended recovery.

On the SZ region formed to dynamically recrystallized grain due to plastic deformation by probe stirring effect.

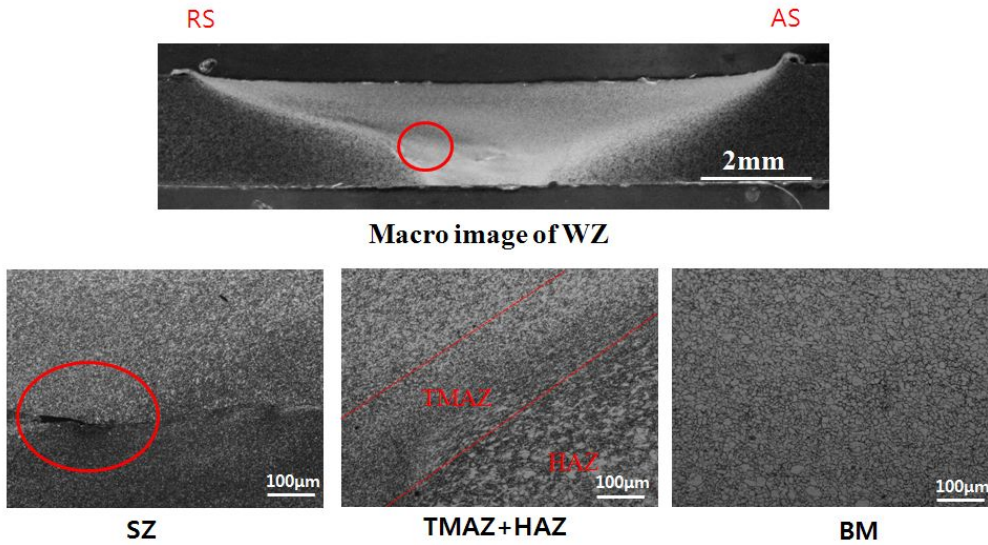
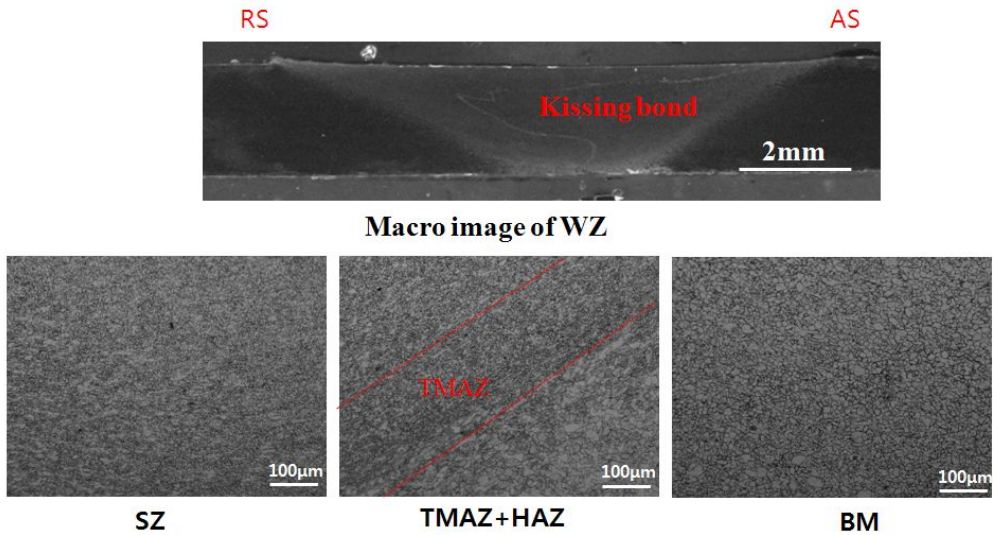


Fig. 4.7 Microstructure of friction stir welded SS400 on rotating speed 400RPM and traveling speed 8mm/s

Fig. 4.7 shows microstructure of friction stir welded SS400 on rotating speed 400RPM and traveling speed 8mm/s. Semicircle like weld zone was formed in comparable with weldzone on traveling speed 3mm/s. It was considered that Heat input decreased with increasing traveling speed. defect was observed in weld zone. As the observation result of optical microscopy, grain size of the BM evaluated about 10~20  $\mu\text{m}$ . However, On the HAZ region was observed to grain coarsening in comparable with BM. Defect was found in bottom of retreating side.





**Fig. 4.8 Microstructure of friction stir welded SS400 on rotating speed 600RPM and traveling speed 8mm/s**

Fig. 4.8 shows microstructure of friction stir welded SS400 on rotating speed 600RPM and traveling speed 8mm/s. No defect was observed in weld zone. As the observation result of optical microscopy, grain size of the BM evaluated about 10~20  $\mu\text{m}$ . However, On the HAZ region was observed to grain coarsening in comparable with BM. Between SZ and HAZ could be observed TMAZ region.

On the SZ region formed to recrystallization of grain due to plastic deformation by probe stirring effect. The author could observe kissing bond on the SZ region. As the result of tensile test, specimen made at rotating speed 600RPM and traveling speed 8mm/s was fractured in the BM. It is considered that Kissing bond could not be affected to decrease of mechanical property.

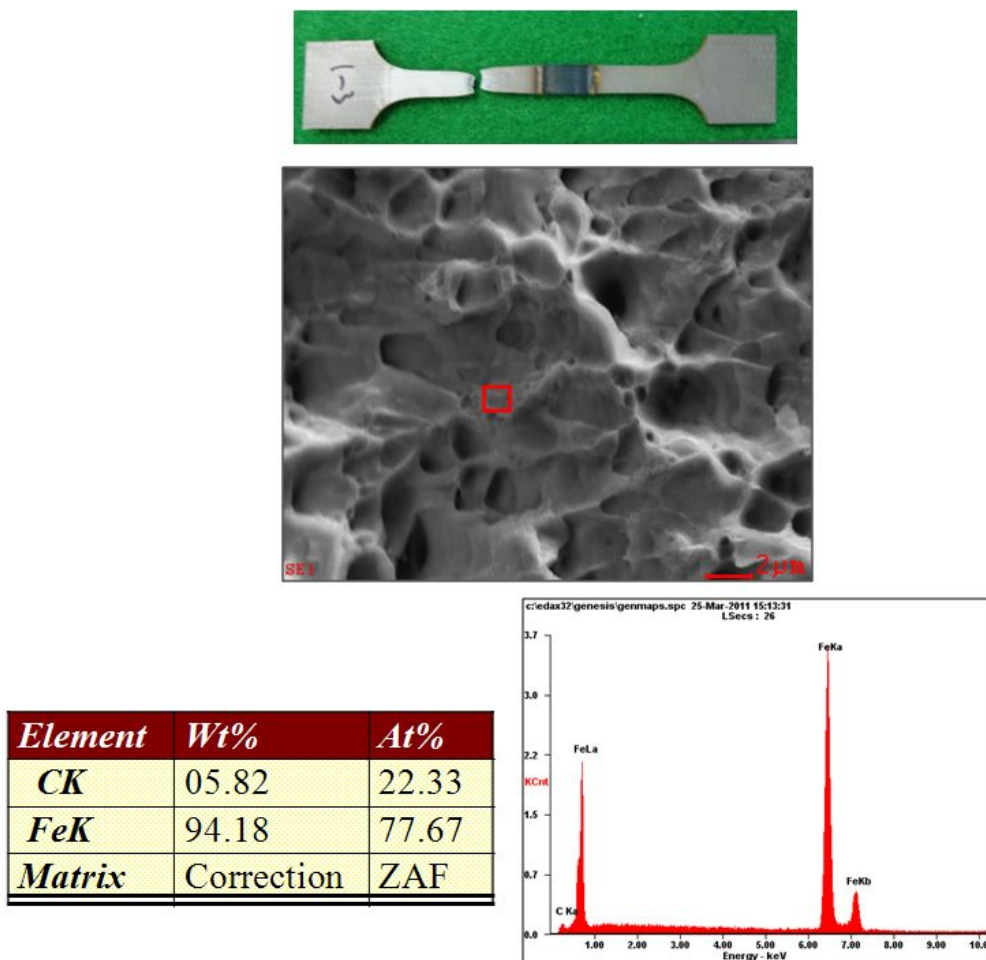


Fig. 4.9 SEM observation of fracture surface and EDAX result\_BM

After tensile test, fracture surface was observed by SEM. Fracture sections exhibit different aspect each welding condition. Fig 4.9 shows SEM observation and EDAX result of fracture surface. Dimples were observed in the fracture zone of BM. It thought that ductile fracture occurred in the BM. As the result of EDAX, C and FE was detected about 05.82 and 94.18 Wt%, respectively.



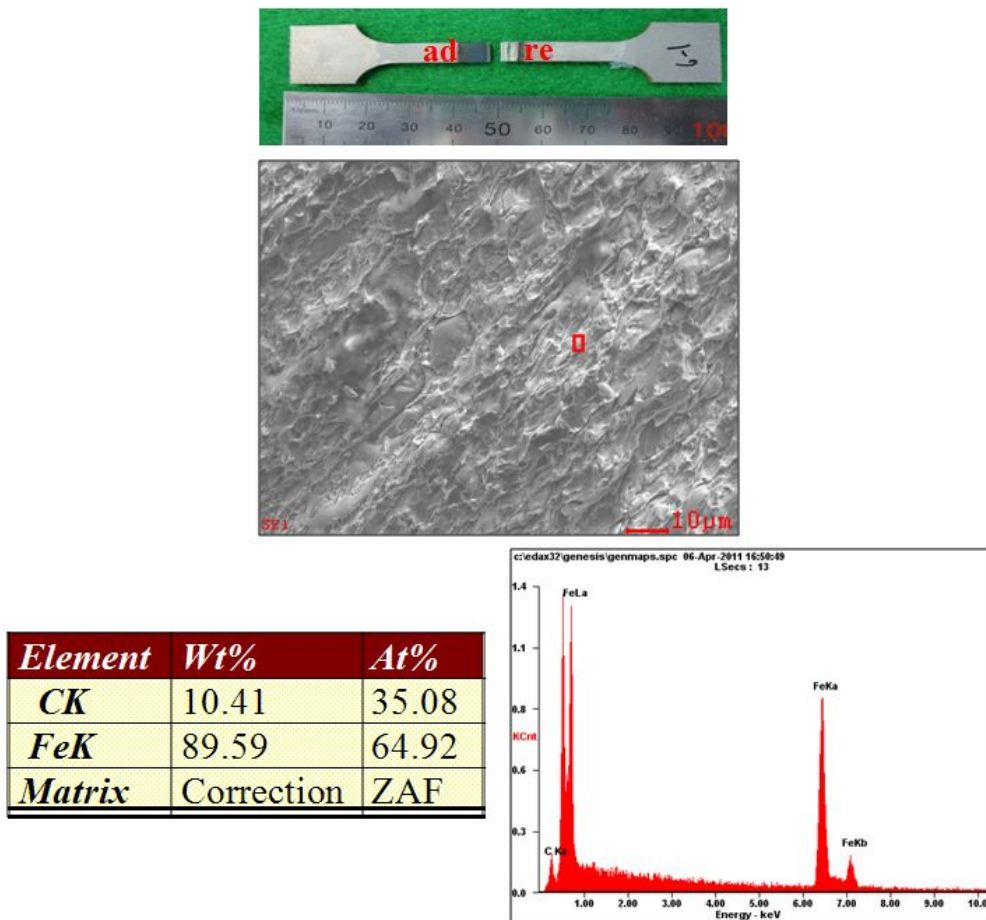


Fig. 4.10 SEM observation of fracture surface and EDAX result\_weld zone

Fig 4.10 shows SEM observation and EDAX result of fracture surface in the weld zone. The weld zone was occurred to brittle fracture. The fracture sequence was complicated in accordance with welding condition.

As the result of EDAX, C and FE was detected about 10.41 and 89.59Wt%, respectively.

## Chapter 5 Conclusion

Friction stir welding was successfully carried out to join typical structure steel(SS400). In order to investigate the weldability of friction stir welds, mechanical properties(tensile test, hardness test) and microstructural analysis have been carried out. From the present study could obtain result as follow;

►The friction stir welding sheet fabricated by rotating speed 600RPM have better mechanical properties than that of rotating speed 400RPM

- In case of welding which was conducted by rotating speed 400RPM and traveling speed 8mm/s, no defect was found in welding appearance. However, as the result of microstructure analysis, defect was observed to bottom in retreating side.

-There is no defect in the friction stir welds that was fabricated on rotating speed 600RPM

-The hardness profile can be seen to be more or less symmetric about the weld interface. There is a significant drop in hardness in the HAZ and TMAZ regions. On the rotating side, the TMAZ hardness was found to be higher than the HAZ hardness. In the SZ, considerable increase in hardness was found compared to HAZ.

-As the result of tensile test, specimen made at rotating speed 600RPM and traveling speed 8mm/s was fractured in the BM. It is considered that Kissing bond could not be affected to decrease of mechanical property.

## REFERENCES

- [1] H.S. Bang, H.S. Bang, S.M. Joo, "Numerical simulation of Al-SPCC weldment", Key Engineering Materials, P1738~1744, Oct., 2006
- [2] Y.J.Chao, and X.Qi: Heat transfer and thermo-mechanical analysis of Friction Stir joining of Al6061-T6 plates, 1st International Symposium on Friction Stir Welding, (1999).
- [3] A.Askari, S.Silling, B.London, and M.Mahoney: Modelling and Analysis of Friction Stir Welding Processes, Friction stir welding and Processing, TMS publication,(2001) p.43.
- [4] H.S. Bang. "Study on The Mechanical Behaviour of Welded part in thick Plate - Three-dimensional Thermal Elasto-Plastic Analysis Baseon Finite Element Method." Journal of the Korean Welding Society, Vol.10, No.4, pp.37~43, December 1992.
- [5] G.H. Jeon, A Study on Weldability of TIG Assisted Friction Stir Dissimilar Welding of Al6061 Alloy and STS Sheet, 2010
- [6] Ulrike Dressler, Gerhard Biallas, Ulises Alfaro Mercado. "Friction stir welding of titanium alloy Ti6Al4V to aluminium alloy AA2024-T3", 2009
- [7] AWS, WELDING HANDBOOK, Vol.1, Eighth Edition, 1987.
- [8] AWS, WELDING HANDBOOK, Vol.2, Eighth Edition, 1991.
- [9] Bynum, J.E., "Modification to the Hole Drilling Technique of Measuring Residual Stresses for Improved Accuracy and Reproducibility", Journal of Experimental Mechanics, U.S.A., Vol. 21, No. 1, Jan. 1981.
- [10] Hidekazu Murakawa, Jianxun Zhang and Hiroyuki Minami, "FEM Simulation of welding process(ReportIII)", Trans. JWRI, Vol. 28, No.1, pp.41~46, 1999.
- [11] L.E.Murr, et al.: Solid-state flow association with the friction stir welding of dissimilar metals, Fluid flow phenomena in metals

processing (1999), 31-40

- [12] Z. Sun, R. Karppi, "The application of electron beam welding for the joining of dissimilar metals: an overview", Journal of materials processing technology 59 (1996) 257-267
- [13] H.S. Bang, G.Y. Han, "The plane-deformation thermal elasto-plastic analysis during welding of plate", The society of naval architects of korea p33~40, Apr.1994
- [14] WELDING HANDBOOK, Eighth Edition, Volume 3, MATERIALS AND APPLICATION PART 1, pp.100~110, AMERICAN WELDING SOCIETY.
- [15] E. G. WEST, THE WELDING OF NON-FERROUS METALS, CHAPMAN & HALL LTD, 1951, pp.129~254.

## Part 2

### Chapter 1. Introduction

#### 1 . 1 Background & Purpose

High performance and concurrent weight and cost reduction become more important in almost industries. Therefore the demand for dissimilar metal joining has been increased in many industrial fields including transportation systems and electronics. As an implication there is a need for a welding method allowing for joining dissimilar materials such as Ti and Al that high strength, low weight and low cost are characterized. In the case of aerospace industry, the joining of Al alloy and Ti alloy could have a major application in the body structure where high strength and light weight are desirable. Especially Titanium and Ti alloys are widely used because of their high corrosion resistance and high specific strength. Several access to weld aluminum and titanium have been made in the past. Conventional fusion welding methods such as arc and laser welding have been tried. Unfortunately, however, sound joints with acceptable strength have not been obtained because of the formation of intermetallic compounds in weld region and/or weld interface. And all these representative examples exhibited problems like the necessity for shielding gas, sophisticated equipment and geometrical limitations of the welding interface.

The welding institute(TWI) was developed friction stir welding process in 1991. FSW is a solid-state joining technique in which a rotating tool is traversed along the weld path, plastically deforming the surrounding material to form the weld and generating significant heat around the tool during FSW[14]. Since its development in 1991, the friction stir weld process has increased acceptance as a joining method of choice for industry such as automotive, shipbuilding, aerospace using aluminum alloy.

In the present study, dissimilar materials joints between AA6061-T6

and Ti-6Al-4V sheets were fabricated by using friction stir welding method. Microstructure and mechanical properties of weld zone was examined. Especially, the interfacial microstructure and element distribution was precisely investigated by STEM.

## Chapter 2. Experimental procedure

Five millimeters-thick sheets of Ti-6Al-4V alloy and A6061-T6 alloy were successfully friction stir welded using 2-dimensional precision FSW machine. The chemical composition and mechanical properties of the base materials were listed in Table1 and Table2, respectively.

**Table 2.1 Chemical composition of AA6061-T6 and Ti-6Al-4V base metals (at%)**

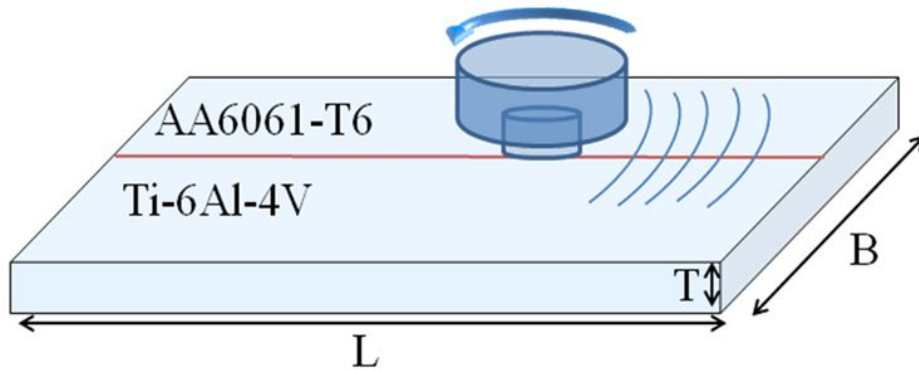
	Si	Mg	Cu	Fe	C	V	Others	Al	Ti
6061-T6	0.56	0.98	0.31	0.29	-	-	0.09	Bal.	-
Ti-6Al-4V	-	-	-	0.40	0.10	3.95	0.04	6.62	Bal.

**Table 2.2 Mechanical properties of AA6061-T6 and Ti-6Al-4V base metals**

	YS(Mpa)	UTS(Mpa)	El.(%)
6061-T6	310	342	17
Ti-6Al-4V	880	950	14

The butt joining was carried out using a FSW tool consisting of tapered from 6mm at the probe root area to 4mm at the probe tip area with a screw. The shoulder diameter and probe length is 15mm and 4.5mm, respectively. The tool was made of standard steel(SKD61). Butt joints were made along the RD of the sheet with tool traveling speed of 2.5mm/s and tool rotation speed of 1000RPM. During the FSW, 3° tilt angle and a plunge depth of 0.2mm were applied to the tool.

Fig. 2.1 shows a schematic illustration of friction stir welding process between AA6061-T6 and Ti-6Al-4V. During FSW, advancing side is Al



alloy and retreating side is Ti alloy.

**Fig. 2.1 Schematic illustration of friction stir welding process between AA6061-T6 and Ti-6Al-4V**

Contrary to conventional friction stir butt welding, the tool probe center was nearly shifted by the probe radius towards the aluminum plate. Therefore, except for a few tenth millimeter, the stirring action of the probe occurred on the aluminum plate of the joint. This was conducted to prevent probe wear and over heating of the aluminum alloy. This welding process was similar to the FSW of steel-aluminum joints.

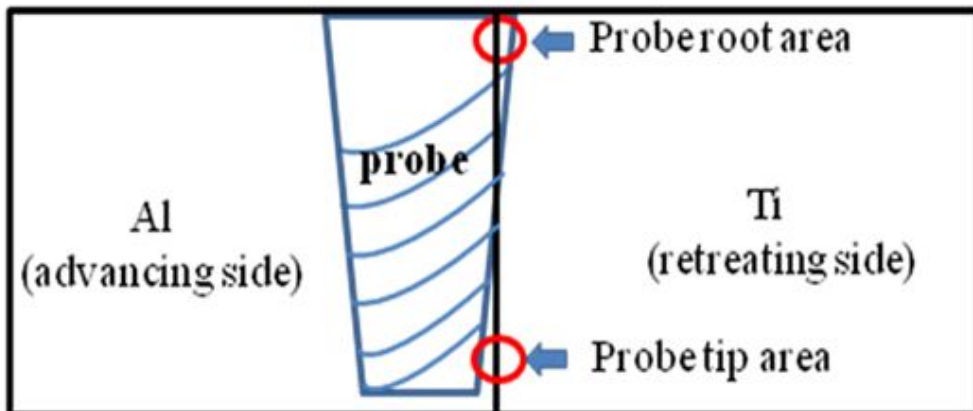


**Fig. 2.2 Schematic illustration of joint interface**

Fig. 2.2 shows a schematic illustration of joint interface. To evaluate



interfacial microstructure and mechanical properties in accordance with the probe position, probe positions were varied along thickness direction of base metals. Probe root area was equivalent to the weld surface and the probe was completely inserted in Ti-alloy of this region. However, probe tip area was equivalent to to the weld bottom and the probe was not contact to Ti-alloy. Interfacial microstructure was inspected by optical microscopy(NIKON, EPIHOT200), scanning electron microscopy(JEOL, JSM-700F) and scanning transmission electron microscopy(FEI, TECNAI); sections taken perpendicular to the welding direction were polished and etched(keller's reagent) by using conventional methods. TEM specimens on a cross-section perpendicular to welding direction were fabricated by focused ion beam(FEI, QUANTA3D). The bright field images of the weld interface were observed. The high angle annular dark field(HAADF) images were observed and consequently elements mapping was carried for the same field. Tensile test was carried out by using an instron-type tester under a cross head speed of 1.7xm/s at room temperature. Tensile test specimens (gage length: 45mm, width: 7.5mm) were machined perpendicular to the welding direction from joint. After tensile test, fracture surfaces were inspected by a scanning electron microscopy equipped with X-ray spectroscopy analysis system(EDX). Vickers hardness profiles were measured each of 0.05mm from Ti sheet to Al sheet using indenter and a load of 490mN. And hardness test were conducted on a cross-section  $1/4t$  perpendicular to the welding direction.

## Chapter 3. Result and discussion

### 3.1 Mechanical properties

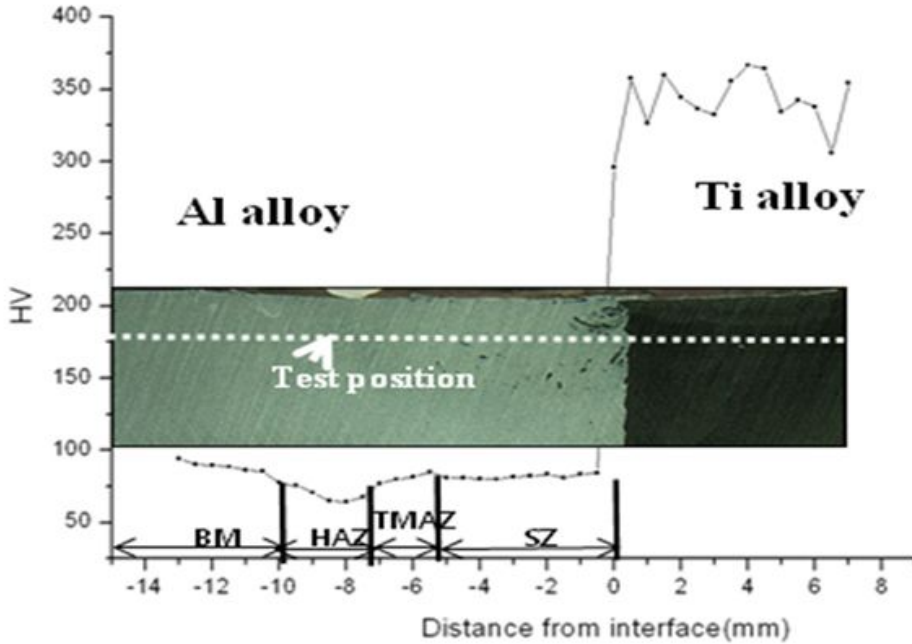


Fig. 3.1 Hardness profile for the welding cross-section

Hardness profile for the welding cross-section evaluated by Vickers hardness tester is shown in Fig. 3.1. The hardness level of Ti-6Al-4V side amounts to circa 350HV. Sharp decrease of hardness level generated at the stir zone. Hardness level of stir zone is slightly smaller than that of Al alloy base metal, except when the indenter hited titanium particles. HAZ has a lowest hardness level. It is considered that annealing effect of HAZ was caused by friction heating. The stress-strain curves of the tensile test specimens are shown in Fig. 3.2 The ultimate tensile strength reached 134Mpa representing 35% by that of Al alloy base metal. The all joints expressed lower strength and elongation than base metal. This is because probe tip area could not be

affected by probe stirring action. The all joints are fractured in the weld region during transverse tensile test.

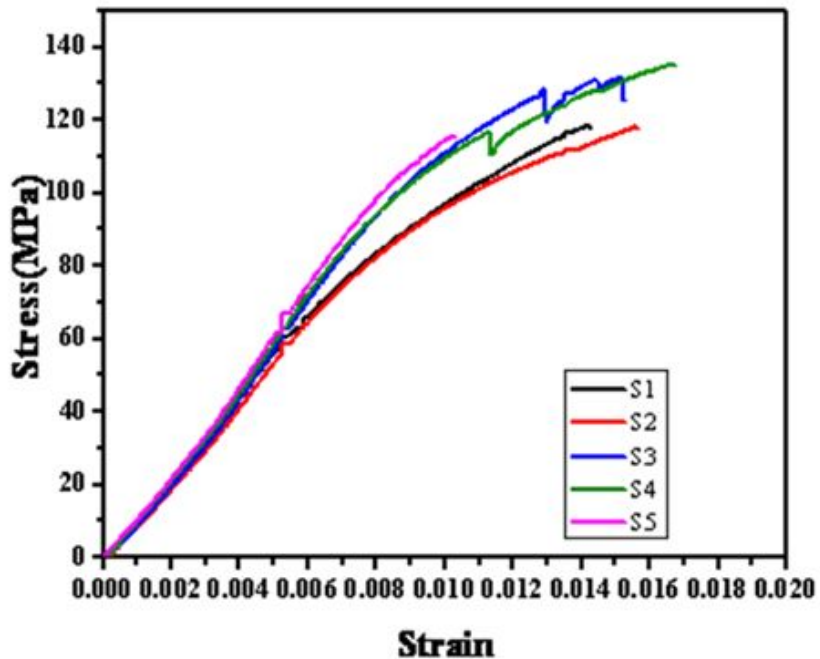
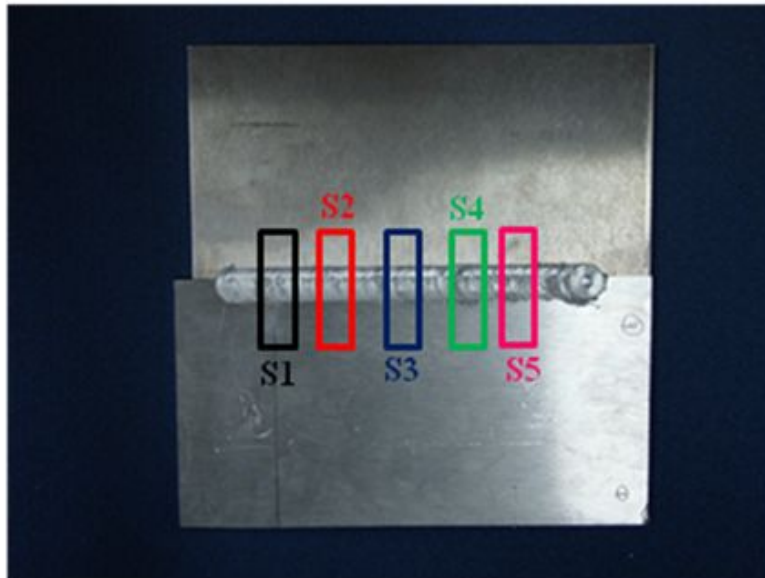


Fig. 3.2 Strain–Stress curve of friction stir welds between and AA6061–T6 and Ti–6Al–4V

## 3.2 Interfacial microstructure

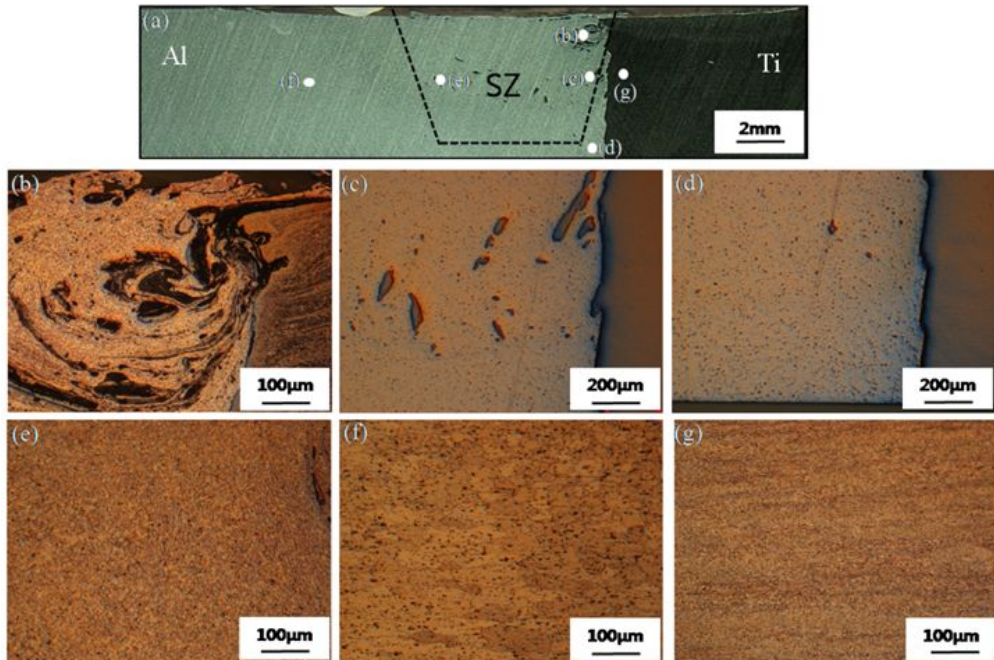
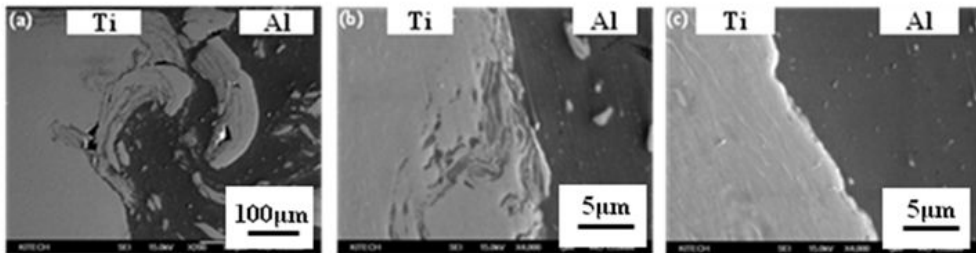


Fig. 3.3 The cross-section image of friction stir welded AA6061-T6 and Ti-6Al-4V(a) and the optical microscopy(OM) images of the cross-section(b-g).

Fig. 3.3 shows that the cross-section image of friction stir welded AA6061-T6 and Ti-6Al-4V(a) and the optical microscopy(OM) images of the cross-section(b-g). The stir zone occurs mainly on the aluminum side of joint. Because tool was shifted towards AA6061-T6, SZ was formed mostly on the AA6061-T6 of the weld zone. Ti-6Al-4V fragments were observed in SZ. SZ was composed of finely recrystallized Al alloy grains and Ti alloy fragments pushed away from the titanium base metal due to the stirring effect of the probe. Therefore SZ has a composite structure of aluminum alloy reinforced by titanium particles. Middle area of the weld interface evaluated by OM is shown in Fig. 3.3(c). Ti alloy fragments were also observed in SZ.

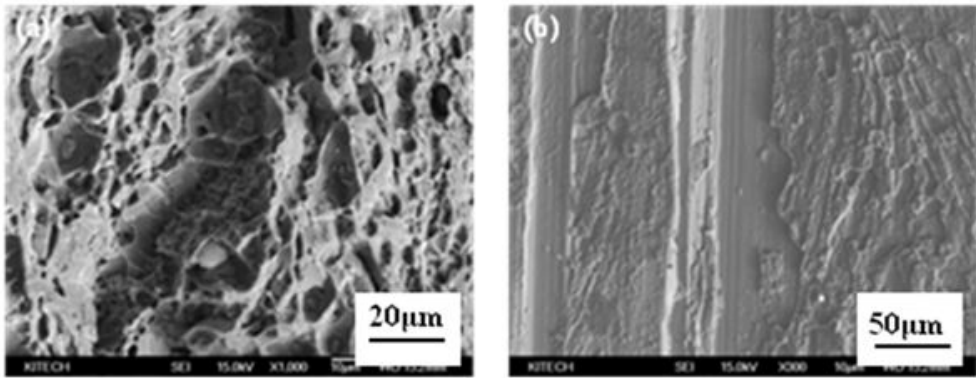
However, they were not found in the probe tip area of the weld interface (Fig. 3.3(d)). This is why the probe did not stir the Ti alloy in direction. Crystal grains of the Al alloy in SZ (Fig. 3.3(e)) became significantly fine compared with the initial grain size of Al alloy base metal (Fig. 3.3(f)). Fig. 3.3(g) shows Ti alloy base metal around the weld interface. It was not affected by the stirring action of the probe during FSW.



**Fig. 3.4 SEM images of probe root area(a), middle area(b), tip area(c) in the weld interface**

Fig. 3.4 shows SEM images of the weld interface. Lots of coarse fragment of Ti alloy were observed in the probe root area, Fig. 3.4(a). It thought that the strong stirring was occurred in this region. In the middle area, small fragment of the Ti alloy and the particles of the Al alloy were observed, Fig. 3.4(b). No evidence of the stirring action by the probe was found in the probe tip area of the weld interface, Fig. 3.4(c). This reason was expressed above, already. And irregular lamellar structures were formed in interfacial zone due to plastic flow of base metal by probe stirring action. After tensile test, fracture surface was observed by SEM. Fracture sections exhibit different aspect along the plate thickness direction. Fig. 3.5(a) is for the probe root area, dimples were observed. It thought that ductile fracture occurred on the probe root area. As the result of EDAX analysis of Fig. 3.5(a), these area

**Fig. 3.5 SEM images for fracture surface (a) and probe tip area (b)**



display an aluminum content of about 100%. From this result, it is considered that the fracture of this region occurred in SZ of Al alloy. In the probe tip area, the initial surface of Ti alloy sheet was observed. it was confirmed that the fracture sequences are very complicate and the fracture position depends on the probe position.

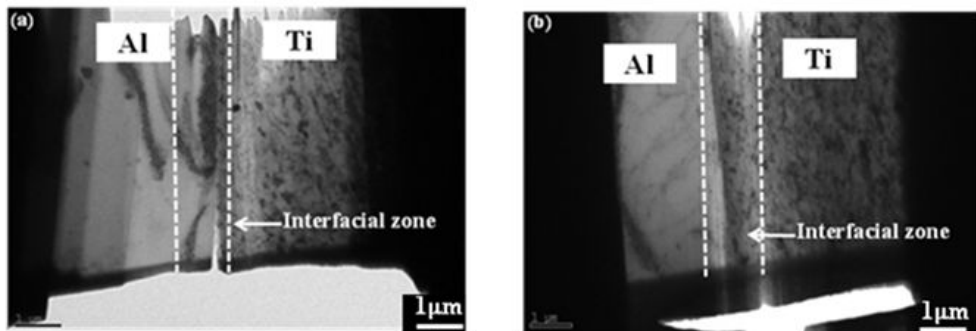


Fig. 3.6 TEM specimens fabricated by FIB

TEM specimens fabricated by FIB are shown in Fig. 3.6. Interfacial zone could be observed in these specimens. Fig. 3.7 shows bright filed images of probe root area and probe tip area. In the weld interface of probe root area, wavy morphological interface was observed at Al alloy side. It is considered that the wavy morphology was formed by spiral fabrication in the surface of probe. However, the wavy morphology was



not observed at the weld interface in the probe tip area. This is because of effect from the tool with circular truncated shape. Ti alloy of probe tip area could not contact with probe.

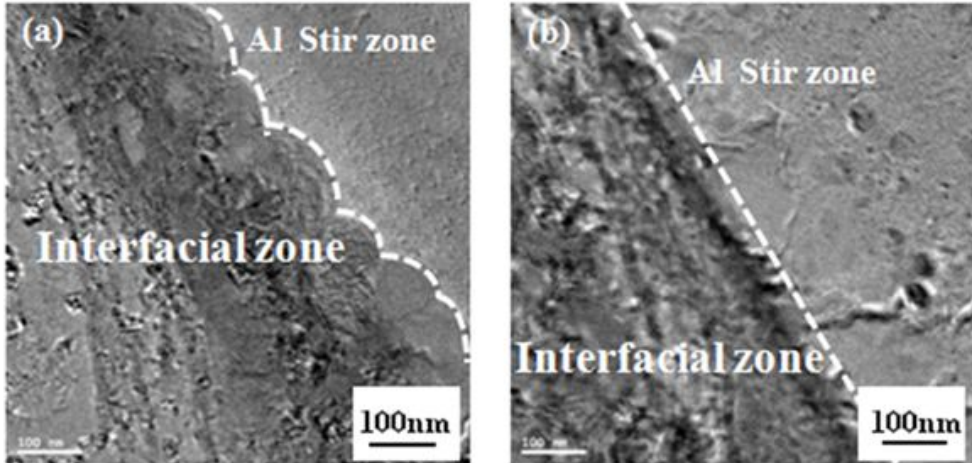


Fig. 3.7 bright dark filed images of probe root area(a) and probe tip area(b)

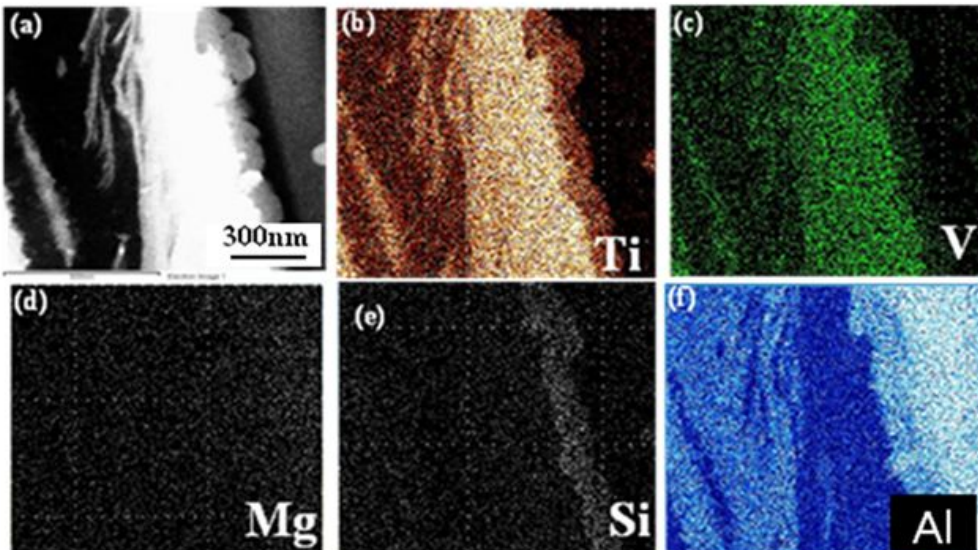


Fig. 3.8 High angle annular dark field(HAADF) images and elements mapping of probe root area in FSW welds

High angle annular dark field(HAADF) images and elements mapping of

probe root area in FSW welds are shown in Fig. 3.8.

Various contrasts were detected at the interfacial zone along thickness direction in HAADF images. It thought that composition of interfacial zone did not be homogenous and specified compositions were concentrated irregularly at interfacial zone. In bright area with 500nm width in HAADF image, Ti and V element was concentrated at the weld interface and Al element was concentrated at the dark area. As the result, It was considered that metal flow caused by stirring action of high rotation tool was resulted in lamellar structure. Intermetallic compound which was observed in the fusion weld zone was not found in the present weld interface. It was considered that friction stir weld process of the present study did not occur in melting and solidification. At the Irregular lamellar and/or feather-like distribution of Al, Ti and V component was also detected. However, it did not found special trend to Mg distribution. According to the elements mapping result, Si was concentrated at the weld interface having wavy morphology. The HAADF image and elements mapping of probe tip area are also shown in Fig. 3.9. In the probe tip area, wavy morphological interface was not observed. However, weak concentration of Si component was detected at the weld interface along the sheet thickness direction.



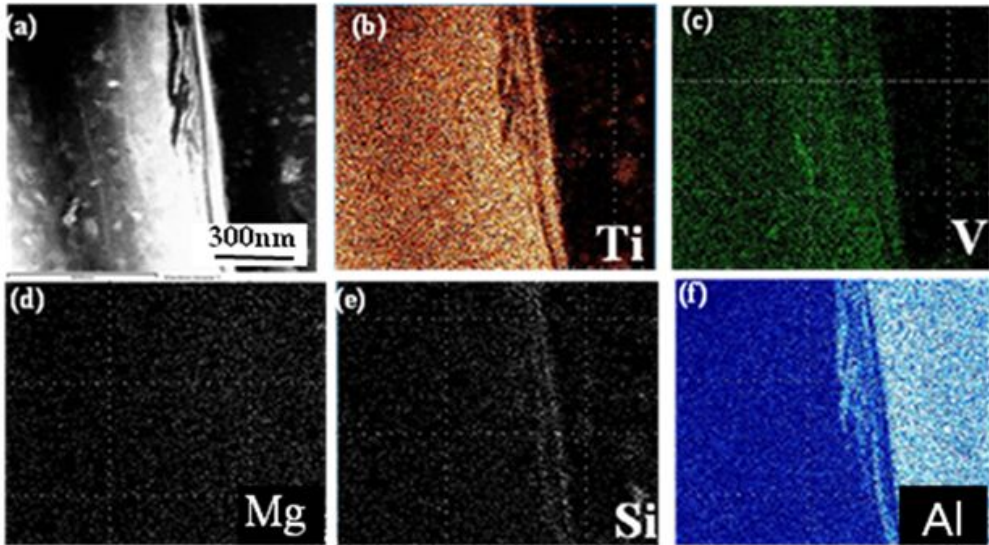


Fig. 3.9 HAADF image and elements mapping of probe tip area

## Chapter 4. Conclusion

In the present study, butt joining of AA-6061T6 and Ti-6Al-4V plates was performed using a 2-dimensional precision friction stir welding machine. The morphology of the interfacial zone formed between SZ of Al alloy and the edge of Ti alloy was examined. A morphological investigation and element mapping analysis were precisely evaluated for the interfacial zone. The mutual relationship between the probe position and interfacial microstructure was investigated and the following results were made clear.

In the probe root area, the SZ reveals finely recrystallized grains of Al alloy and fragments of Ti alloy formed by the contact and consequent stirring between the front of Ti alloy plate and the inclined flank of the probe. Dimples of Al were observed at the fracture surface by tensile test in this case. This suggests that the weld interface between the edge of the SZ and the front of Ti alloy was sound. The formation of wavy morphological interface was also confirmed. It is considered that this was due to spiral work on the flank of probe. According to the TEM-HAADF verification and element mapping analysis, it was confirmed that the weld interface reveals very complicate sequence including lamella structure with Al and Ti-V. Feather-like distribution of Ti-V component was also detected. In the probe tip area, however, the initial front (and/or surface) of Ti alloy plate was observed. It thought that actual joining reaction was not occurred in the present area and this resulted in the strength decrease.

In conclusion, it was clearly revealed that mechanical properties and interfacial microstructure of AA6061-T6/Ti-6Al-4V but joints manufactured by FSW are affected by the probe position. Further, it was also confirmed that the probe must be shifted toward Ti alloy plates to get sound joints.

## REFERENCES

- [1] Ulrike Dressler, Gerhard Biallas and Ulses Alfaro Mercado: *Materials Science and Engineering A*. 526(2009)113–117
- [2] Y.C.Chen and K.Nakata: *Materials and Design*. 30(2009)469–474
- [3] Yu Zhang, Yukata S. Sato, Hiroyuki Kokawa, Seung Hwan C. Park, Satoshi Hirano: *Materials Science and Engineering A* 488 (2008) 25–30
- [4] J.Q. Su, T.W. Nelson, R. Mishra and M. Mahoney: *Acta materialia*. 51 (2003) 713–729
- [5] Kh. A.A. Hassan, A.F.Norman, D.A. Price, P.B.Prangnell: *Acta Materialia* 51 (2003) 1923–1936
- [6] Won-Bae Lee, Chang-Young Lee, Woong-seong Chang, Yun-Mo Yeon, Seung-Boo Jung: *Materials Letters* 59 (2005) 3315–3318
- [7] Bangcheng Yang, Junhui Yan, Michale A. Sutton, Anthony P.Reynolds: *Materials Science and Engineering A* 364 (2004) 55–65
- [8] M.Peel, A.Steuwer, M.preuss, P.J Withers: *Acta Materialia* 51 (2003) 4791–4801
- [9] ] L.Zhou, H.J.Lin, P.Liu, and Q.W.Liu: *Scripta Materialia*. 61(2009)596–599
- [10] ]Yu Zhang, Yutaka S. Sato, Hiroyuki kokawa, Seung Hwan C. Park, Satoshi Hirano: *Mater Science and Engineering A* 485(2008) 448–455
- [11] K.V Jata and S.L. Semiatin: *Scripta mater*. 43(2000) 743–749
- [12] S.Mironov, Y.Zhang, Y.S.Sato and H.Kokawa: *Scripta Materialia* 59 (2008) 511–514
- [13] YUTAKA S, HIROYUKI KOKAWA, MASATOSHI ENOMOTO and SHITETOSHI JOGAN: *Metall. Mater. Trans. A* 30(1999) 2429–2437
- [14] R.W.Fonda, J.F.Bingert, K.J.colligan: *Scripta Materialia* (2004) 243–248

## 저작물 이용 허락서

학 과	선박해양공학과	학 번	20107325	과 정	석사
성 명	한글: 방기상 한문: 房基相 영문: Bang, Ki-Sang				
주 소	서울시 중랑구 목1동 109-6번지				
연락처	E-MAIL : qkdrltk@lycos.co.kr				

논문제목	<p>한글 : 고용점 소재에 대한 마찰교반용접부의 기계적성질 및 미세조직</p> <p>영어 : Mechanical properties and microstructure of Friction stir welds for high melting temperature materials</p>
------	---

본인이 저작한 위의 저작물에 대하여 다음과 같은 조건아래 조선대학교가 저작물을 이용할 수 있도록 허락하고 동의합니다.

- 다 음 -

1. 저작물의 DB구축 및 인터넷을 포함한 정보통신망에의 공개를 위한 저작물의 복제, 기억장치에의 저장, 전송 등을 허락함
2. 위의 목적을 위하여 필요한 범위 내에서의 편집·형식상의 변경을 허락함. 다만, 저작물의 내용변경은 금지함.
3. 배포·전송된 저작물의 영리적 목적을 위한 복제, 저장, 전송 등은 금지함.
4. 저작물에 대한 이용기간은 5년으로 하고, 기간종료 3개월 이내에 별도의 의사 표시가 없을 경우에는 저작물의 이용기간을 계속 연장함.
5. 해당 저작물의 저작권을 타인에게 양도하거나 또는 출판을 허락을 하였을 경우에는 1개월 이내에 대학에 이를 통보함.
6. 조선대학교는 저작물의 이용허락 이후 해당 저작물로 인하여 발생하는 타인에 의한 권리 침해에 대하여 일체의 법적 책임을 지지 않음
7. 소속대학의 협정기관에 저작물의 제공 및 인터넷 등 정보통신망을 이용한 저작물의 전송·출력을 허락함.

동의여부 : 동의( 0 ) 반대( )

2011 년 5 월

저작자: 방 기 상(인)

**조선대학교 총장 귀하**